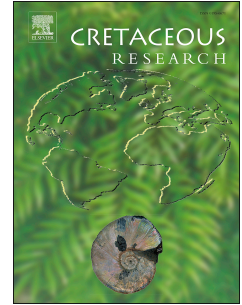


# Journal Pre-proof

An Early Cretaceous, medium-sized carcharodontosaurid theropod (Dinosauria, Saurischia) from the Mulichinco Formation (upper Valanginian), Neuquén Province, Patagonia, Argentina

Rodolfo A. Coria, Currie, Philip J. Currie, Francisco Ortega, Mattia A. Baiano



PII: S0195-6671(19)30395-7

DOI: <https://doi.org/10.1016/j.cretres.2019.104319>

Reference: YCRES 104319

To appear in: *Cretaceous Research*

Received Date: 11 September 2019

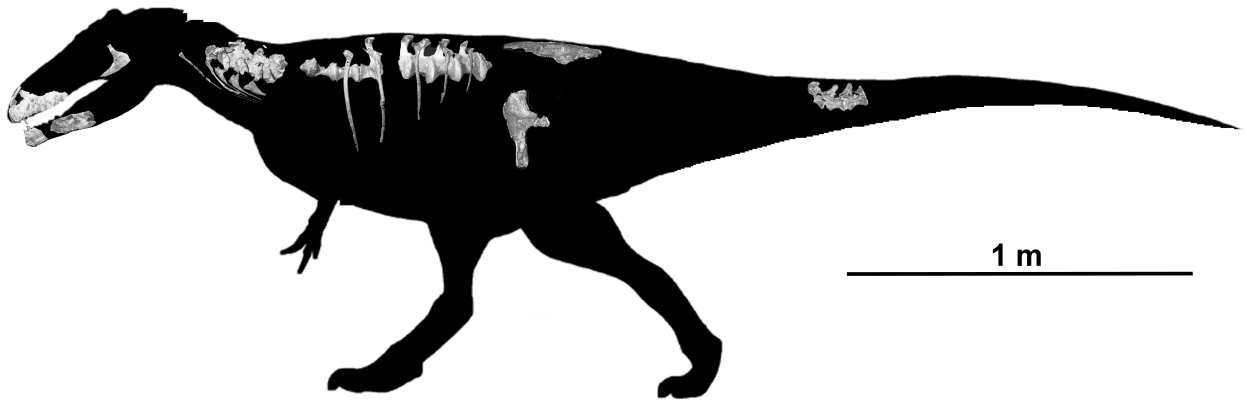
Revised Date: 10 October 2019

Accepted Date: 11 November 2019

Please cite this article as: Coria, R.A., Currie, Currie, P.J., Ortega, F., Baiano, M.A., An Early Cretaceous, medium-sized carcharodontosaurid theropod (Dinosauria, Saurischia) from the Mulichinco Formation (upper Valanginian), Neuquén Province, Patagonia, Argentina, *Cretaceous Research*, <https://doi.org/10.1016/j.cretres.2019.104319>.

This is a PDF file of an article that has undergone enhancements after acceptance, such as the addition of a cover page and metadata, and formatting for readability, but it is not yet the definitive version of record. This version will undergo additional copyediting, typesetting and review before it is published in its final form, but we are providing this version to give early visibility of the article. Please note that, during the production process, errors may be discovered which could affect the content, and all legal disclaimers that apply to the journal pertain.

© 2019 Elsevier Ltd. All rights reserved.



Journal Pre-proof

1 **An Early Cretaceous, medium-sized carcharodontosaurid theropod (Dinosauria,**  
2 **Saurischia) from the Mulichinco Formation (upper Valanginian), Neuquén Province,**  
3 **Patagonia, Argentina**

4

5 Rodolfo A. Coria<sup>a</sup>, Currie, Philip J. Currie<sup>b</sup>, Francisco Ortega<sup>c</sup>, Mattia A. Baiano<sup>a,d</sup>

6 <sup>a</sup> CONICET – Museo Carmen Funes, Av. Córdoba 55, (8318) Plaza Huinca, Neuquén,  
7 Argentina. [rcoria@unrn.edu.ar](mailto:rcoria@unrn.edu.ar); [mbaiano@unrn.edu.ar](mailto:m baiano@unrn.edu.ar)

8 <sup>b</sup> University of Alberta, Biological Sciences CW405, Edmonton, Alberta T6G 2E9, Canada.  
9 [pjcurrie@ualberta.ca](mailto:pjcurrie@ualberta.ca)

10 <sup>c</sup> UNED, Fac. de Ciencias. Senda del Rey 9, 28040. Madrid, Spain. [fortega@ccia.uned.es](mailto:fortega@ccia.uned.es)

11 <sup>d</sup> CONICET-IIPG, Av. Roca 1242 (8322), General Roca, Río Negro, Argentina

12

13

14 Corresponding author: R.A. Coria [rcoria@unrn.edu.ar](mailto:rcoria@unrn.edu.ar)

15

16

17 **Abstract**

18

19 A new carcharodontosaurid taxon, *Lajasvenator ascheriae* gen. et sp. nov. is described. The new  
20 taxon is based on two specimens: MLL-PV-Pv-005 is a partial skeleton represented by a portion of the  
21 snout, partially articulated presacral vertebral series, four articulated caudal vertebra and fragments of the  
22 pelvic girdle; MLL-PV-Pv-007 includes the anterior ends of both dentaries, a quadratojugal, and  
23 fragments of cervical vertebrae, ribs and a possible tarsal bone. *Lajasvenator* is unique in having anterior  
24 projections on cervical prezygapophyses, lip-like crests on the lateral surfaces of cervical  
25 postzygapophyses, and bilobed anterior processes on cervical ribs. *Lajasvenator* material was collected  
26 from the terrestrial sandstones of the Valanginian Mulichinco Formation. It is the oldest  
27 carcharodontosaurid record from South America. This medium sized theropod was found associated with  
28 remains of the dicraeosaurid sauropod *Pilmatueia*, indeterminate diplodocid remains, and a yet  
29 unidentified iguanodontian-like ornithopod.

30

31 Keywords: *Lajasvenator*; Carcharodontosauridae; Theropoda; Valanginian; Patagonia

32

## 1. Introduction

During the second half of the 20th Century, knowledge about South American dinosaur faunas was primarily built upon a wealth of discoveries from the Mesozoic outcrops of Argentina (see Coria, 2016; Ezcurra and Novas, 2016; Salgado and Calvo, 2016, and references therein). Notwithstanding, most dinosaur taxa are known from the latest levels of the Cretaceous, given the scarcity of Lower Cretaceous outcrops.

In a global context, fossil-bearing localities from the lowest levels of the Cretaceous -- the Berrasian and Valanginian -- are either scarce or have uncertain stratigraphic identification (Weishampel et al., 2004). A handful of Valanginian dinosaur species are known from Asia, Australia and Europe, although the phylogenetic status of many of these species is currently uncertain (Broom, 1904; Buffetaut et al., 2009a and b; Carpenter and Ishida, 2010; Christiansen and Bonde, 2003; Galton, 2009; Harrison and Walker, 1973; de Klerk et al., 2000; Norman, 2010, 2012; Pereda-Suberbiola et al., 2012; Rauhut and Xu, 2005; Taylor and Naish, 2007; You et al., 2005).

In Argentina, the Valanginian is well exposed in the Neuquén Basin, where it is represented by marine and terrestrial deposits of the Mulichinco and Bajada Colorada formations (Gulisano et al., 1984; Zavala, 1999, 2000), which are considered to be synchronous, at least at some of their levels. The Mulichinco Formation includes older beds composed mostly of marine deposits, whereas the upper terrestrial sediments are unconformably overlain by the marine sediments of the Agrio Formation (upper Valanginian–lower Barremian) (Zavala et al., 2005).

Since 2009, annual expeditions have collected fossil vertebrates at the locality of Pilmatué, located 9 km northeast from Las Lajas, Neuquén Province. Here, the terrestrial levels of the Mulichinco Formation are extensively exposed over many square kilometers. Through the years, numerous dinosaur remains have been collected, including articulated or semiarticulated skeletons of dicraeosaurid sauropods, ornithopods and theropod dinosaurs (Coria et al., 2010, 2012, 2017, 2019; Paulina Carabajal et

58 al., 2018), many of which are associated with fossil plants (Martinez et al., 2012; Gnaedinger et al., 2017).  
59 Furthermore, recent collections of vertebrate fossils from the synchronous Bajada Colorada Formation  
60 produced what could be a similar dinosaur association (Gallina et al., 2014, 2019; Canale et al., 2017),  
61 suggesting that the fossils from both formations could represent the same ecosystem.

62 During the 2010 field season at Pilmatué locality, a partial, semiarticulated skeleton of a medium  
63 sized theropod (MLL-Pv-005) was collected (Fig.1). A second, less complete specimen (MLL-Pv-007)  
64 was recovered 50 meters southeast from the same stratigraphic level during the 2012 field season, which  
65 although very incomplete, it preserved the proximal end of a cervical rib that is undistinguishable from  
66 the seventh cervical rib of the specimen MLL-Pv-005. A new theropod taxon – *Lajasvenator ascheriae*  
67 gen. et sp. nov. – is based on these materials, which constitutes the first theropod remains reported for the  
68 Valanginian Cretaceous of Patagonia (Coria et al., 2010) and the first described Theropoda taxon from the  
69 Mulichinco Formation (Fig.1).

70 *Lajasvenator* shows clear features that link it with the Carcharodontosauridae, a clade of meat-  
71 eating dinosaurs commonly known by large, heavily built, Late Cretaceous forms like *Giganotosaurus*,  
72 *Carcharodontosaurus*, *Mapusaurus* and *Tyrannotitan* (Coria and Salgado, 1995; Coria and Currie, 2006;  
73 Novas et al., 2005; Sereno et al., 1995). However, little is known from the early stages of the evolution of  
74 the clade, which could be represented by medium size species like the one here described. *Lajasvenator* is  
75 the oldest Cretaceous carcharodontosaurid from South America and a key element to understand the  
76 evolutionary history of this clade, which could be older than thought for this continent.

77

## 78 2. Institutional abbreviations:

79 IVPP, Institute of Vertebrate Paleontology and Paleoanthropology, Beijing, China; MCF-PVPH, Museo  
80 Municipal Carmen Funes, Vertebrate Paleontology, Plaza Huincul, Neuquén Province, Argentina; MLL-  
81 PV, Museo Municipal de Las Lajas, Las Lajas, Neuquén Province, Argentina; MPCA PV, Museo

82 Provincial Carlos Ameghino, Vertebrate Paleontology, Cipolletti, Río Negro Province, Argentina;  
83 MUCPv-CH, Museo de la Universidad Nacional del Comahue, El Chocón Collection, Neuquén City,  
84 Argentina; USNM, United States National Museum, Washington DC, USA.

85

### 86 **3. Systematic Paleontology**

87

88 Theropoda Marsh, 1881

89 Tetanurae Gauthier, 1986

90 Allosauroidea Currie and Zhao, 1993

91 Carcharodontosauridae Stromer, 1931

92

93 *Lajasvenator ascheriae* gen. et sp. nov.

94 Etymology: *Lajas*, referring the city of Las Lajas, within the jurisdiction of which the specimen  
95 was found; *venator*, Latin, hunter; *ascheriae*, after Susana Ascheri, for her kindness in allowing  
96 us to work on her land.

97 Holotype: MLL-PV-005, an incomplete but partially articulated skeleton that includes a partial  
98 skull represented by the almost complete left premaxilla with one tooth, anterior portion of the  
99 right premaxilla with two teeth, most of the main body of the left maxilla, anterior section of the  
100 main body of the right maxilla, distal half of the left dentary, posterior ramus of the left splenial,  
101 complete last four cervical vertebrae (articulated with each other and their cervical ribs), almost  
102 complete first dorsal vertebra, a series of nine articulated dorsal centra (the centra are incomplete  
103 at the anterior and posterior ends of the series), fragment of sacrum with three incomplete

104 vertebrae attached to a fragmentary ilium, a series of four articulated mid caudal vertebrae (two of  
105 which are complete), five almost complete posterior dorsal ribs with heads, three dorsal rib shaft  
106 fragments, four fragments of possible gastralia, incomplete right ilium, and proximal end of the  
107 right pubis.

108 Referred material: MLL-PV-007, a right quadratojugal, symphysial ends of both dentaries,  
109 fragmentary series of four cervical transverse processes, proximal end of seventh right cervical  
110 rib, proximal half of a left, anterior dorsal rib, and a possible distal tarsal.

111 Locality and horizon: Pilmatué Locality, 9 km northeast of Las Lajas, Neuquén Province,  
112 Patagonia, Argentina. Mulichinco Formation (upper Valanginian, Lower Cretaceous). GPS  
113 positions: MLL-PV-005, S38° 29' 59.5", W70° 15' 51.1", Elevation 732 masl; MLL-PV-007,  
114 S38° 29' 59.6", W70° 15' 48.0", same elevation as MLL-PV-005. (Figs. 2 and 3).

115 Diagnosis: medium-sized theropod with the following autapomorphies: anterior projection on  
116 cervical prezygapophyses, lip-like crest on lateral surface of cervical postzygapophyses, and  
117 cervical ribs with bilobed anterior process. The phylogenetic analysis shows that *Lajasvenator*  
118 has the following unique combination of features: premaxilla ventral to external naris has a  
119 height/length ratio less than 0.5 (character 2); paracaudal plates with striated or ridged surfaces  
120 (character 140); relatively small premaxillary teeth (character 152); cervical vertebrae with a  
121 distinct rim on each anterior articular surface (character 175) (all characters are also present in  
122 some megalosaurs); and ilium with straight dorsal margin (also in some basal theropods).

123

#### 124 **4. Description**

125 The holotype (MLL-PV-005) consists in an adult individual based on the complete fusion  
126 of neural arches with their respective central along the preserved vertebral elements. The partial  
127 skull was lying on its left side and was upside down in relation to the hips and posterior dorsal



128 vertebrae. The neck was twisted downwards so that the distal elements of the cervical vertebrae  
129 and their ribs were recovered in articulation. The hips and posterior part of the abdomen were  
130 lying on the right side when the animal was buried, and most of the left side of this region was  
131 destroyed by erosion. This suggests that the animal was articulated when buried, and was in a  
132 modified death pose. It was collected from a heavily indurated, coarse-grained sandstone layer,  
133 and had been eroding for a long time before it was discovered and excavated.

134         Premaxilla. The left premaxilla is complete, whereas the right one lacks the supranarial  
135 process and the posterior end (Fig. 4). Both premaxillae were recovered in contact but were not  
136 fused with each other, or with the maxillae.

137         The external surface of the left premaxilla is somewhat weathered, but that of the right  
138 premaxilla is relatively smooth other than pitting for nutrient foramina (Fig. 4A). The subnarial  
139 body of the premaxilla is somewhat taller (43 mm) than long (41 mm anteroposteriorly, 43 mm  
140 obliquely between the front and back of the alveolar margin). There are four alveoli in each  
141 premaxilla. The last alveolus is positioned under the front of the external naris. The supranarial  
142 process arches high above the external naris and the posterior end is 90 mm above the alveolar  
143 margin of the maxilla. The external naris was clearly large (about 30 by 60 mm) with a  
144 posterodorsally inclined axis. On the left side, the premaxilla has a tapering, elongate  
145 posterodorsal, subnarial process, which is more clearly seen in medial view. It separates the  
146 maxilla from the narial margin and probably contacted the subnarial process of the nasal.

147         Maxilla. The anteroventral region of the left maxilla is preserved with the first seven  
148 alveoli (Table 1) (Fig. 4). The external surface of the bone is heavily weathered in most places. In  
149 areas where the outer surface is well-preserved, there are anteroventrally trending canals and  
150 deeply rugose texture that are characteristic of carcharodontosaurids like *Giganotosaurus*  
151 (MUCPv-CH-01) and *Mapusaurus* (MCF-PVPH-108), and abelisaurids like *Aucasaurus* (MCF-

152 PVPH-236). The anterior ramus is as long as it is deep, and extends beneath the posterior region  
153 of the external naris. Neither the posterodorsal (lacrimal) process nor the interfenestral region is  
154 preserved. However, depressions in the dorsal surface of the palatal shelf show that there were  
155 pneumatic excavations in the anterior ramus. A curved edge on the medial surface of the anterior  
156 border of the antorbital fossa presumably marks the position of the promaxillary fenestra.  
157 However, because the posteromedial margin of the promaxillary fenestra is not preserved, it is  
158 impossible to know if the fenestra was exposed in lateral view. The ventral margins of the  
159 antorbital fossa and fenestra seem to coincide in the posterior region of the preserved part of the  
160 left maxilla. The interdental plates are texturally distinct from the medial alveolar margin, and  
161 have patterns of vertical ridges and grooves. The first interdental plate is small and low (9 mm),  
162 but subsequent ones increase progressively in height. The tallest plate (25 mm) is between the  
163 fourth and fifth alveoli. Posterior to this one, they are fused into a continuous plate that decreases  
164 steadily in height. The fused interdental plates resemble those of *Acrocanthosaurus* (Eddy and  
165 Clark, 2011), *Carcharodontosaurus* (Stromer, 1931), *Eocarcharia* (Sereno and Brusatte, 2008),  
166 *Giganotosaurus* (MUCPv-CH-1), *Mapusaurus* (MCF-PVPH-108, Coria and Currie, 2006) and  
167 other carcharodontosaurids, but also abelisaurids (Lamanna et al., 2002; Sampson and Witmer,  
168 2007), *Allosaurus* (Madsen, 1976), *Ceratosaurus* (Madsen and Welles, 2000), dromaeosaurids  
169 (Currie, 1995), *Torvosaurus* (Britt, 1991) and many other theropods.

170         Quadratojugal. MLL-Pv-007 includes a nearly complete right quadratojugal (Fig. 5).

171         It has an “L” shape, with dorsal and anterior rami forming a 90° angle. The dorsal ramus  
172 lacks the distal end, but it is more slender and thinner than that in *Allosaurus* (Madsen, 1976).  
173 The posterior side of the dorsal ramus has a shallow depression that would have formed the  
174 anterolateral border of a large quadratic fenestra. On the medial surface of the quadratojugal,  
175 below the quadratic fenestra, is a tall, rugose facet that would have contacted the lower end of the  
176 quadrate (Fig. 5C). The ventroposterior end of the quadratojugal is shallowly convex with a small

177 notch that would have exposed a small ventrolateral surface of the quadrate. The anterior ramus is  
178 wide at its base and tapers anteriorly to a single point that would have been wedged between two  
179 posterior prongs of the jugal as in *Acrocanthosaurus* (Currie and Carpenter, 2000) and *Sinraptor*  
180 (Currie and Zhao, 1993). However, unlike the latter, there was no contact for the third, medial  
181 quadratojugal process of the jugal. The sutures for the two prongs of the jugal clearly show that  
182 the upper prong was restricted to the front of the quadratojugal on the dorsal edge, whereas the  
183 lower prong would have been largely overlapped laterally by the quadratojugal but extended  
184 almost to the quadrate suture.

185         Vomers. The anterior parts of the vomers are fused to form a thick midline ridge (17 mm  
186 tall) on the roof of the mouth (Fig. 4D). They contact the premaxillae on the midline anteriorly,  
187 and are held in place posteriorly by the anteriorly tapering anteromedial processes of the maxillae.  
188 The width of the vomer is 12 mm and seems to be constant throughout the preserved part of the  
189 bone. This suggests that the narial region of the animal was narrow.

190         Dentary. Partial dentaries are preserved in the two known specimens of *Lajasvenator*.  
191 MLL-Pv-007 includes the anterior ends of both dentaries, although the right side is slightly more  
192 complete (Fig. 6).

193         The symphyseal ends of *Lajasvenator* have the typical squared-off profile of  
194 carcharodontosaurids, and each has an anteroventral chin-like process (Brusatte and Sereno,  
195 2007; Calvo and Coria, 2000; Currie and Carpenter, 2000; Eddy and Clarke, 2011). The lateral  
196 surfaces of the dentaries are lightly sculptured by grooves and foramina. The first three  
197 neurovascular foramina are close to the dorsolateral edge of the lateral surface, but are not within  
198 a neurovascular groove as they are in *Acrocanthosaurus* (Eddy and Clarke, 2011). However, there  
199 is an anteroposteriorly oriented groove on the ventral edge of the lateral side. It is suspected that  
200 the anterior end of the dorsal neurovascular groove may have been behind the fourth alveolus as it

201 is in *Giganotosaurus* (Calvo and Coria, 2000). In medial view, the proximal end of the Meckelian  
202 groove (Figs. 6D and E) reaches the level between the second and third dentary teeth. The first  
203 three interdental plates are triangular and did not contact each other (Fig. 6E). However, this may  
204 have been an age- or size-specific character because the anterior interdental plates of one of the  
205 smaller specimens of *Mapusaurus* (MCF-PVPH-108.125, Coria and Currie 2006, fig. 8D) and  
206 *Giganotosaurus* (MUCPv-CH-01) are also unfused. Only external sections of three dentary tooth  
207 crowns (second to fourth) are preserved with the right dentary, although the root of the first  
208 dentary tooth can be seen in the broken anterodorsal corner of the bone. Only part of the first  
209 tooth crown is represented on the left dentary, although at least two more alveoli are present with  
210 broken tooth roots.

211 MLL-Pv-005 includes the posteroventral end of the left dentary (Fig. 7). The fragment is  
212 a mediolaterally thin and dorsoventrally deep lamina that is invaded by a distinct oval anterior  
213 extension of the mandibular fenestra on the ventroposterior border. Below the mandibular  
214 fenestra, the ventral border of the dentary is gently convex, wrapping around the ventral edges of  
215 the splenial and probably the angular.

216 Splenial. Part of the posterior ramus of the left splenial of MLL-Pv-005 is  
217 preserved in articulation with the medial side of the dentary, which bears a forked end for the  
218 articulation with the angular (Fig. 8).

219 The long slender shape of the posteroventral process is similar to that of *Mapusaurus*  
220 (MCF-PVPH-108.179), which also forks (Coria and Currie 2006, fig. 9), although at a relatively  
221 more anterior level. The elongate, distally forked process is also found in *Acrocanthosaurus*  
222 (Eddy and Clarke, 2011). The posterodorsal process is rather square in contrast with the triangular  
223 process seen in most theropods.

224           Teeth. Alveoli in the holotype show that there were four premaxillary teeth and at least  
225 seven maxillary teeth (Table 1).

226           Three premaxillary teeth are preserved in their sockets; two in the right premaxilla, which  
227 occupy the third and fourth positions, and one in the left premaxilla that occupies the fourth  
228 position. Each is lateromedially compressed and gently curved. However, each of the three teeth  
229 is oval in basal outline.

230           Predepositional weathering has made details of the carinae and denticulation hard to see.  
231 The anterior carina of the third premaxillary tooth on the right side is offset to the medial side of  
232 the crown (so that the tooth is J-shaped in cross-section) and extends at least half the height of the  
233 crown. Under high magnification, barely discernible denticulation suggests there were 2.7  
234 anterior denticles per millimeter in the apical third of the tooth. The posterior carina has about  
235 three low denticles per millimeter. The enamel of the crown is smooth, and lacks any longitudinal  
236 ridging, striations or crenulations. The alveoli suggest that the first premaxillary tooth was the  
237 smallest, followed by the second. The third premaxillary tooth was the largest, and the fourth is  
238 only slightly smaller. Alveolar size shows that the first maxillary tooth was about the size of the  
239 posterior premaxillary teeth, and that the fifth maxillary tooth would have been the largest tooth.  
240 Maxillary teeth must have been quite bladelike because the widths of the maxillary alveoli are  
241 only about 40% their anteroposterior lengths.

242           The dentary teeth of MLL-Pv-007 are poorly preserved (Fig. 6B and E). Nevertheless, a  
243 few of the serrations can be seen on the posterior carinae of the second and third, right dentary  
244 teeth. The third dentary tooth has a base that is longer anteroposteriorly than wide, and is apically  
245 curved.

246

247 Postcranial

248           The *Lajasvenator* vertebral column is incomplete and represented by articulated partial  
249 series of five cervical, nine dorsal, three sacral and four caudal vertebrae (Table 2).

Journal Pre-proof

250 The most anterior are an articulated series of five vertebrae and ribs (Fig. 9). Based on  
251 comparisons with *Allosaurus* (Madsen, 1976) and *Neovenator* (Brusatte et al., 2008), they correspond to  
252 the 6<sup>th</sup>, 7<sup>th</sup>, 8<sup>th</sup>, 9<sup>th</sup> and 10<sup>th</sup> presacral vertebrae (which are the last four cervicals and the first dorsal). The  
253 dorsal section is represented by an articulated series of the last nine vertebral centra. The sacrum is  
254 preserved partially from the second to the fourth sacral centra, whereas the tail is represented by four  
255 articulated mid-caudal vertebrae. None of the recovered ribs are fused to the vertebrae.

256 Cervical vertebrae: The four cervical centra have concave (anteroventrally and transversally)  
257 ventral surfaces between the parapophyses. They have hemispherical anterior intervertebral articulations,  
258 and strongly opisthocoelous posterior articular surfaces. Each of the preserved cervical vertebrae has  
259 epipophyses, but they are most prominent in the sixth cervical.

260 The most anterior element of the cervical series is identified as a sixth cervical vertebra (Fig. 10).  
261 It is largely destroyed by erosion, but still preserves most of the centrum and tips of both  
262 postzygapophyses. The centrum is longer than high and has deeply excavated lateral sides.

263 The parapophyses on the anteroventral margins of the centrum are well developed and extend  
264 ventrolaterally on short pedicles to a level lower than the anteromedial edge of the centrum (Fig. 10A and  
265 B). In anterior view (Fig. 10B), the broken surface anterior to the left parapophysis reveals that the  
266 interior of the centrum is camellate. Above each parapophysis there is an oval pleurocoel. The deeply  
267 concave posterior intervertebral articulation of the centrum is wider than high (Table 2). The  
268 postzygapophyses are posterodorsally oriented and have well-developed epipophyses represented as small  
269 horn-like processes that project posteriorly. The articular facets of the postzygapophyses face  
270 ventrolaterally. In dorsal view, the lateral edge of each postzygapophysis projects laterally as a  
271 pronounced wing-like process (lappet) with a convex outline. The dorsal surfaces of the  
272 postzygapophyses merge towards the midline and presumably there was a well-developed lamina that  
273 delimited a deep postspinal fossa that can be seen above the neural canal. There is no hyposphene.

274           The seventh cervical is virtually complete (Fig. 11). The centrum is slightly shorter than that of  
275 the sixth cervical (Table 2), but is wider at the midlength constriction. The pleurocoel above each  
276 parapophysis is subdivided by a thick septum into two openings. In anterior view, the prezygapophysial  
277 facets face dorsally and slightly anteromedially. The prezygodiapophysial lamina is well developed and  
278 extends anteriorly beyond the articular facet as a distinct anterior process. This seems to be an  
279 autapomorphic character.

280           On the left side, the wall of the supporting ridge has collapsed to expose the camellate condition  
281 of the prezygapophysis. The articular facet of the prezygapophysis extends both laterally and medially on  
282 distinct lappets. In anterior view, the prezygodiapophysial lamina merges ventromedially with the  
283 centroprezygapophyseal lamina. The prespinal fossa is deep and ventrally limited by  
284 intraprezygapophyseal laminae, which also roof deep anterior peduncular pleurocoels, one on each side of  
285 a midline lamina. In lateral view, the diapophysis is supported by the anterior and posterior  
286 centrodiaophysial laminae that separate the infraprezygapophysial, infradiaophysial and  
287 infrapostzygapophysial fossae. All three fossae are deep and probably extend into the inside of the bone  
288 through pneumatopores. In ventral view, there are distinct lateral and medial lappets that extend the  
289 articular surfaces of the postzygapophyses. In posterior view, the intrapostzygapophysial laminae form a  
290 V-shaped ventral boundary for the postspinal fossa, and roof over a pair of posterior peduncular  
291 pleurocoels. The interspinal ligament scarring covers distinct facets on the anterior and posterior surfaces  
292 of the neural spine. There is neither a hyosphene nor a hypantrum.

293           In most features, the eighth cervical vertebra is similar to the preceding vertebra although is  
294 slightly larger in most dimensions (Fig. 12). There are no peduncular pleurocoels. The anterior prong  
295 beneath the prezygapophyses is more pronounced and there is a conspicuous hemihyosphene beneath  
296 each postzygapophysis.



297           The ninth cervical centrum is marginally larger than its predecessor (Fig. 13). Like the other  
298 preserved cervicals, it has a broad, relatively flat ventral surface that is nevertheless slightly concave  
299 between the parapophyses, and slightly convex posteriorly. There is a low, barely conspicuous midline  
300 ridge behind the level of the parapophyses. The hypantrum is well-developed between the  
301 prezygapophyses, and the interspinous ligament scar extends from the hypantrum to almost the tip of the  
302 neural spine.

303           There is neither a prespinal fossa, nor anterior peduncular pleurocoels. The prezygapophyses  
304 only extend a short distance anterior to the transverse processes. The anterior edges of the  
305 prezygapophyses are not well preserved, but seem to lack the distinctive anterior prongs seen on the two  
306 preceding vertebrae. Posteriorly, the interspinous scar occupies most of the posterior surface of the neural  
307 spine and there is no postspinal fossa. The postzygapophysis on the left side is damaged laterally, but the  
308 one on the right side extends laterally with a distinct epiphysial process that is continuous with the  
309 lateral lappet. The hyosphene articulations are no longer separate, but are connected near the neural  
310 spine by a lamina that is ventrally depressed on the midline. There are no posterior peduncular  
311 pleurocoels.

312           Only the anterior part of the first dorsal (presacral 10) is preserved, including most of the neural  
313 arch (Fig. 14).

314           The postzygapophyses and the posterior half of the centrum are missing. The anterior  
315 intervertebral articulation of the centrum is markedly less convex than it is in the preceding cervicals. The  
316 parapophyses are midheight on the centrum, and unlike the situation in the cervicals, the ventral edge of  
317 the anterior intervertebral articulation is below the rib articulations. There appears to have been a weak  
318 hypapophysis on the midline, and it is strongly offset from the lateral sides of the centrum by deep  
319 depressions. The hypapophysis extends posteriorly as a ventral, midline ridge. There is a large  
320 pneumatopore behind the parapophysis. A ridge on the lateral side of the base of the neural spine extends

321 to the posterodorsal tip of the diapophysis. The latter seems to roof over a complex network of laminae  
322 and pneumatic sinuses that extend into the base of the neural spine.

323 The last nine dorsal vertebrae of MLL-Pv-005 are preserved in articulation, although their left  
324 sides, the neural arches, and some of the midsections (dorsals 15, 19, 23) of the centra were destroyed by  
325 erosion (Fig. 15).

326 The ends of the right diapophyses of the 18<sup>th</sup> to 22<sup>nd</sup> presacrals were preserved in position,  
327 although the shafts of transverse processes were all destroyed by erosion. They were, however,  
328 represented by impressions in the rock. The amphiplatyan centra of all of these dorsals are strongly  
329 waisted, similar to other small allosauroids (Malafaia et al., 2016). This is most extreme in presacrals 16  
330 to 18 (Table 2) in which the ventral surfaces of the centra narrow into sharp medial ridges. None of these  
331 centra appear to have had pneumatopores. The transverse processes are elongate rectangles that project  
332 laterally, dorsally and slightly posteriorly. The ventral surfaces of the distal regions of at least the 19<sup>th</sup> to  
333 21<sup>st</sup> transverse processes have what are presumed to be pneumatic fossae.

334 Parts of three fused sacral vertebrae were recovered with MLL-PV-005. The anterior and  
335 posterior vertebrae of the triad are incomplete. However, the arrangement of transverse processes and  
336 sacral ribs suggests that these are the second, third and fourth sacrals. The centrum of the third sacral is  
337 approximately 68 mm long, and is pierced on both sides by pneumatopores with diameters of more than a  
338 centimeter. The sacral rib attachments between the second/third, and third/fourth centra are fused to the  
339 centra, although the sutures are still visible. The transverse processes of the third and fourth sacral  
340 vertebrae sweep outwards and backwards. The neural arches are broken, but the bases are thin and  
341 bladelike.

342 Four articulated caudal vertebrae were recovered (one represented by only the postzygapophyses  
343 and part of the neural spine) (Fig. 16).

344           The three well-preserved caudals have conspicuous, wide transverse processes and must be from  
345 the middle of the tail. Transverse processes can go far back in caudals of carcharodontosaurids -- at least  
346 30 in *Acrocanthosaurus* (Harris, 1998) – but the sizes of the transverse processes and the dimensions of  
347 the central suggest that the caudals of MLL-Pv-005 are probably from the region of the 15<sup>th</sup> to 20<sup>th</sup>  
348 caudals. Presumably the caudals between the sacrum and this section were present when the animal was  
349 buried because their alignment follows a natural curve from the hips that would be appropriate for a  
350 typical death pose with the tail curved forwards dorsal to the hips. However, the caudal vertebrae did not  
351 continue in the rock beyond this preserved section of four vertebrae. None of the preserved caudal centra  
352 has a ventral midline sulcus, nor is there any evidence of pleurocoels. The absence of a sulcus is  
353 characteristic of *Neovenator* and derived carcharodontosaurids (Brusatte et al., 2008), whereas it is  
354 present in *Veterupristisaurus* (Rauhut, 2011) and *Concavenator* (Ortega et al., 2010). The facets for the  
355 haemal arches seem to be equally developed on the front and back of each centrum. The neural arch is  
356 indistinguishably fused to the centrum in each of the caudals, and is taller than the height of the centrum  
357 (Table 2). The neural spine inclines dorsoposteriorly so that the distal (dorsal) end is positioned above the  
358 front of the succeeding vertebra. The midline ridge of the neural spine extends forward until it rises into a  
359 small but distinct spinous process (accessory neural spine) as in *Acrocanthosaurus* (Currie and Carpenter,  
360 2000; Harris, 1998; Stovall and Langston, 1950), *Allosaurus* (Gilmore, 1920), *Dubreuillosaurus* (Allain,  
361 2005), *Mapusaurus* (Coria and Currie, 2006), *Sinosauroptryx* (Currie and Chen, 2001) and a few other  
362 theropods. However, accessory neural spines have been reported in rauisuchians (Franca et al., 2011) and  
363 probably have little taxonomic utility. The prezygapophyses are relatively elongate, and extend somewhat  
364 more than a third of the length of the preceding centrum. Articular facets on the zygapophyses are nearly  
365 vertical in orientation. The transverse process of the second preserved caudal is split into a double  
366 process. It is assumed that this represents a pathological condition because the transverse processes of the  
367 following two vertebrae are more typical rectangular plates that are orientated laterally and slightly  
368 posteriorly.

369 MLL-Pv-007 has only fragments of four vertebrae that were clearly articulated until they were  
370 mostly destroyed by erosion. They appear to be the ends of transverse processes from cervicals or anterior  
371 dorsals. The sizes of the processes and the degree of separation suggest they were from an animal about  
372 the same size as MLL-Pv-005.

373 The longest of the most anterior pair of preserved cervical ribs of MLL-Pv-005 consists of long  
374 and thin rods of bone, of which the one from the left side is 25,5 cm long. It probably represents most of  
375 the shaft of the fifth cervical rib. Nothing from the proximal end is preserved.

376 The next cervical ribs of the preserved series correspond to the sixth pair (Fig. 17).

377 The rib from the right side seems to be complete and is 26 cm long. It has a conspicuous, bilobed  
378 anterior process that is laterally compressed. In medial view, the articular facet of the capitulum is kidney-  
379 shaped and significantly larger than the facet of the tuberculum. Both capitulum and tuberculum are  
380 linked by a short lamina. The articular facets of the capitulum and tuberculum are separated by about 25  
381 mm, and the anterolateral process extends about 18 mm in front of the capitulum. Although the  
382 anterolateral process is prominent, it is considered short because it does not extend anteriorly beyond the  
383 level of the lateral margin of the intervertebral articulation of the centrum. The shaft is proximally convex  
384 laterally and flattens distally. The shaft tapers distally until the diameter is less than 2 mm. On the mesial  
385 surface, ridges extend between the capitulum-anterior processes and the tuberculum-anterior process, but  
386 there is no evidence of pneumatopores in the depressions on either side of the body.

387 Each of the seventh pair of cervical ribs of MLL-Pv-005 was at least 25 cm long, based on the  
388 more complete right rib. The proximal end is dorsoventrally wider than any of the preceding ribs, and so  
389 is the bilobed anterolateral process. The capitulum and tuberculum articular facets are separated by 30  
390 mm, and the anterolateral process extends 20 mm forward. Pneumatic recesses or pneumatopores  
391 excavate the base of the capitulum on the mesial surface. An incomplete right cervical rib of MLL-Pv-007

392 seems to be from a seventh cervical rib and shows a clear pneumatic recess behind the ridge joining the  
393 capitulum and tuberculum mesially. There is a pneumatopore anterior to that ridge.

394 The eighth cervical ribs are 22 cm long. The anterior process, which has fingerlike processes,  
395 projects 22 mm in front of the parapophyseal articulation. The capitulum and tuberculum articular facets  
396 are separated by 37 mm, and multiple pneumatopores penetrate the mesial depressions into the otherwise  
397 thick region between the two heads. The distal end of the shaft tapers to a diameter of 3 mm. The rib from  
398 the left side seems to have been broken and re-healed during life of the specimen.

399 The next pair of ribs is associated with the ninth cervical vertebra.. The distance between the  
400 articular facets of the capitulum and tuberculum is 31 mm on the left side, but is 43 mm on the right side.  
401 The ribs are 72 mm in length on the right side and 95 on the left side, but most of their shafts are missing.  
402 The anterior process of the right side projects 17 mm in front of the junction with the ventral head of the  
403 rib, and is bilobed anteriorly. There is a large pneumatopore on the inside of each of these ribs and  
404 another that faces anteriorly near the junction of the capitulum, tuberculum and anterior process.

405 Five of the last six dorsal ribs are preserved on the right side of MLL-Pv-005, and presumably  
406 represent presacral ribs 17, 18, 20, 21 and 22 (Fig. 18).

407 Presacral rib 17, which would be dorsal rib 8, is 35 cm long when measured along the outside  
408 curve between the tuberculum and distal end. The distal end tapers to 6 mm in diameter. Presacral rib 18  
409 was broken but had healed while the animal was still alive. The distance between the capitulum and  
410 tuberculum measures about 8 cm. In spite of the fact that the adjacent vertebrae and ribs are in natural  
411 articulation, there is no sign of any part of rib 19. One can only assume that it was destroyed at the same  
412 time as most of the associated vertebra. Presacral ribs 20, 21 and 22 seem to be complete except possibly  
413 for their distal tips, and measure 25 cm, 21 cm and 17 cm respectively (capitulum to distal end in a  
414 straight line).

415 Up to a dozen fragments of ribs and several gastralia were recovered with ML-005, but provide  
416 little information. The thickest rib fragment, which is 20 cm long, has a minimum shaft diameter of 18  
417 mm (mediolateral) by 14 mm (anteroposterior) and probably is from one of the first dorsal ribs.

418 Most of an anterior dorsal rib was recovered with MLL-Pv-007. It is about 24 cm long, and the  
419 minimum mediolateral shaft width is 21 mm. The separation between the capitular and tubercular  
420 articulations is 48 mm, which is close to what the separation is between the parapophysis and diapophysis  
421 of the first dorsal vertebra of MLL-Pv-005.

422 The right ilium is partially preserved, although it was split longitudinally by a crack that had been  
423 widened by erosion. Assuming that the two blocks that contained the ilium had not moved in relation to  
424 each other, then the distance between the ventral edge of the pubic peduncle and the top of the ilium is  
425 220 mm. The upper edge of the bone is relatively straight in lateral view (Fig. 19).

426 As in most theropods, there are conspicuous but small vertical ridges (striations) on the medial  
427 surface near the edge of the bone (Fig.19B). A fragment of bone adhering to the medial surface is  
428 probably a remnant of the dorsal limit of the third sacral rib. None of the broken surfaces suggest that the  
429 bone was pneumatic as in *Mapusaurus* (Coria and Currie, 2006) or *Murusraptor* (Coria and Currie,  
430 2016), although a relatively small portion of the ilium is preserved. A small fragment anteroventral to the  
431 main iliac fragment seems to be part of the preacetabular process, and suggests that it extended at least 17  
432 cm in front of the anterior margin of the acetabulum, and well beyond the anterior edge of the pubic  
433 peduncle. The pubic peduncle is attached to the head of the pubis, but the contact is visible (especially on  
434 the lateral surface) which suggests that they were not coossified. The distal end of the peduncle is 86 mm  
435 long, and 41 mm wide. A lateral ridge starts on the edge of the acetabulum 34 mm above the pubic  
436 contact, and quickly expands the articular surface of the acetabulum to 54 mm. This is the base of the  
437 antitrochanteric shelf, which would have expanded even more broadly over the anterodorsal region of the  
438 femoral articulation.

439           The 18 cm long proximal fragment of the right pubis is attached to the pubic peduncle of the  
440 ilium (Fig. 20).

441           It is evident from the orientations of its contacts with the ilium and ischium that the shaft of the  
442 bone was almost perpendicular to the longitudinal axis of the ilium as in *Aerosteon* (Serenio et al., 2008),  
443 *Murusraptor* (Coria and Currie, 2016) and *Concavenator* (Ortega et al., 2010). In this and other features,  
444 it resembles the pubis of *Megaraptor* (Calvo et al., 2004) and *Murusraptor* (Coria and Currie, 2016). The  
445 ischial peduncle is somewhat damaged, but clearly was low (41 mm) and short anteroposteriorly (48 mm  
446 from the posterior margin of the pubic shaft). The pubis formed about 4 cm of the acetabular margin,  
447 where it has a smooth dorsal surface that is 27 mm wide. The anteroposterior diameter of the pubic shaft  
448 is 35 mm. The posterodorsal margin of the pubis below the ischial peduncle is similar to the typical  
449 allosauroid condition and does not enclose an obturator foramen (Brusatte et al., 2008). On the medial  
450 surface, the dorsal limit of the pubic apron is 107 mm from the contact with the ilium.

451           A small fragment of the ischium is attached to the ischial peduncle of the pubis. The puboischial  
452 contact seems to have been vertical in orientation.

453           MLL-Pv-007 also includes fragments of the distal end of a metatarsal and other indeterminate  
454 fragments. None of these provided any particularly useful information or measurements to this study.  
455 However, there is also a complete basipodial element (Fig. 21).

456           In outline and most details, it most closely resembles either the radiale of *Allosaurus* (Gilmore 1920,  
457 fig. 45) or the third right distal tarsal of *Sinraptor* (Currie and Zhao, 1993, fig. 24). The bone is 29 mm  
458 long, 21 mm wide and up to 10 mm thick. Comparison of vertebral measurements suggests that  
459 *Lajasvenator* was about half the size of either *Allosaurus* or *Sinraptor*. Given the variability in size of  
460 theropod carpal and tarsal elements, the bone in question has roughly the right size to be either element (it  
461 is 0.71 the size of USNM 4734, an *Allosaurus* radiale, and 0.38 the size of the *Sinraptor* distal tarsal 3 of  
462 IVPP 10600).

463

464 **5. Discussion**

465

466 The phylogenetic relationships of *Lajasvenator* among theropods were analyzed using a character  
467 matrix composed of 367 cranial and postcranial features distributed among 67 theropod taxa. The  
468 character matrix used was based on that one proposed by Coria and Currie (2016), which in turn was  
469 taken, with some modifications, from previous contributions (Carrano et al., 2012; Zanno and  
470 Makovicky, 2013). That character set was extended with additional characters and taxa presented by  
471 Apesteguía et al., (2016) (see Supplementary Material A and B). The character matrix was analyzed using  
472 TNT version 1.5 (Goloboff and Catalano, 2016).

473 Preliminarily, the analysis resulted in 15200 MPTs with 1147 steps in length, with a CI = 0.372  
474 and RI= 0.660. *Lajasvenator* is clearly nested in a basal position within Carcharodontosauridae, in an  
475 unsolved polytomy with *Concavenator* and *Eocarcharia* (Fig. 22) (Supplementary Material C).

476 *Lajasvenator* shares with *Concavenator* the presence of an accessory centrodiapophyseal lamina  
477 in each dorsal vertebra (character 182, unknown in *Eocarcharia*). On the other hand, *Lajasvenator* shares  
478 with gigantosaurines and *Carcharodontosaurus* a maxilla with a sculptured external surface (character  
479 34). Like most carcharodontosaurids, there is an anteroventrally inclined anterior end of junction between  
480 medial wall and parадental plates in the maxilla (character 17, unknown in *Concavenator* and  
481 *Tyrannotitan*). *Lajasvenator* also shares several apomorphies with most allosauroids (except *Allosaurus*),  
482 including parадental plates that lack replacement grooves (character 138), camellate internal structure of  
483 pneumatic centra (character 160), cervical vertebrae that each have an anterior pleurocoel consisting of  
484 two openings oriented anteroventrally and posterodorsally (character 169), anteroposteriorly elongate  
485 cervical pleurocoels (character 170), and a pubic peduncle of the ilium that has a length to width ratio  
486 greater than 2 (character 272).



487           The presence of *Lajasvenator* in the Mulichinco Formation is significant because of the  
488 stratigraphic context of this unit. This new form represents the oldest record of Carcharodontosauridae in  
489 South America. The family has conspicuous diversity at younger levels of the Cretaceous, when it is  
490 represented by large-sized forms like *Giganotosaurus*, *Mapusaurus*, *Tyrannotitan* (Coria and Currie,  
491 2006; Coria and Salgado, 1995; Novas et al., 2005) and indeterminate remains from Brazil (de Azevedo et  
492 al., 2013). *Taurovenator violantei* (Motta et al., 2016) is a recently described carcharodontosaurid taxon  
493 based on an isolated right postorbital. The autapomorphies proposed to support this taxon consist of the  
494 presence of a horn-like prominence on the orbital brow, and a deep excavation on the ventral surface of  
495 the postorbital. However, these features are present in *Mapusaurus* (MCF-PVPH-108.177) and, although  
496 less developed, are also in *Giganotosaurus* (MUCPv-CH-1). The holotype specimen MPCA PV 802 of  
497 *Taurovenator* also exhibits the ventrolateral curved lateral margin of the palpebral (Motta et al., 2016,  
498 figs. 4 and 5), a diagnostic feature proposed for *Mapusaurus roseae* (Coria and Currie, 2006).  
499 Considering that the holotype specimen of *Taurovenator* (MPCA PV 802) was collected at the same  
500 stratigraphic level as *Mapusaurus* (Huincul Formation), and that there are no further autapomorphies in  
501 that single postorbital, it seems more reasonably to consider *Taurovenator violantei* as junior synonym of  
502 *Mapusaurus roseae*.

503           Other Cretaceous carcharodontosaurid records are known from North America, Europe, Africa  
504 and Asia (*Acrocanthosaurus*, *Carcharodontosaurus*, *Concavenator*, *Eocarcharias*, *Sauroniops*,  
505 *Siamraptor* and *Shaochilong*) (Brusatte et al., 2009; Cau et al., 2013; Chokchaloemwong et al., 2019;  
506 D’Emic et al. 2012; Ortega et al., 2010; Sereno and Brusatte, 2008; Sereno et al., 1996). The Jurassic  
507 record of this clade is poorly represented by the African form *Veterupristisaurus milneri* from Tendaguru  
508 (Rauhut, 2011), although have been also referred to Carcharodontosauria some specimens collected from  
509 the Jurassic of Portugal (Malafaia et al., 2017, 2019), and possibly some teeth from the Middle–Upper  
510 Jurassic of the Shishugou Formation of China (Han et al., 2011), and from the Lower Saxony Basin of  
511 Germany (Gerke and Wings, 2016). Although no carcharodontosaurids have yet been recognized from the

512 Jurassic of South America, it is expected that this clade was present on this continent before the  
513 Cretaceous.

514 The faunal association of different dinosaur taxa collected from the Mulichinco Formation  
515 includes *Lajasvenator*, ornithopods, and diplodocid and dicraeosaurid sauropods (Coria et al., 2010, 2019;  
516 Gnaedinger et al., 2017). The association is, up to certain point, comparable with that known from the  
517 Jurassic of Tendaguru (Janensch, 1914; Rauhut, 2011; Remes, 2004). Although the available fossil  
518 evidence is not conclusive, it is conceivable that some Jurassic dinosaur associations may have survived  
519 into Early Cretaceous times. Such a Cretaceous association – formed by dicraeosaurids, diplodocids,  
520 carcharodontosaurid theropods and non-hadrosaurian ornithopods – has to date only been recognized in  
521 the Valanginian of Patagonia. An Early Cretaceous dinosaur association with strong Jurassic roots  
522 preceded the drastic faunal turnover represented by the extinction of these ancient lineages and the  
523 diversification of titanosaur sauropods and abelisaur theropods occurred in the Turonian of South  
524 America (Coria and Salgado, 2005).

525

## 526 6. Concluding Remarks

527

528 The diversity of South American dinosaurs is increased by the first Valanginian record of a  
529 carcharodontosaurid theropod, *Lajasvenator ascheriae*.

530 *Lajasvenator* is also the oldest South American carcharodontosaurid record, suggesting that the  
531 evolutionary history of the clade likely has older roots than was thought.

532 Carcharodontosaurids are typically associated with large predator forms from the Upper Cretaceous  
533 Gondwanan beds, and in some way, were considered as ecological equivalents to the Laurasian  
534 tyrannosauroids. The new taxon, *Lajasvenator ascheriae*, is based on a medium-sized adult individual,  
535 indicating that Carcharodontosauride, as a group, is more diverse than previously considered.

## 536 Acknowledgments

537 MLL-Pv-005 was found by the first author in 2009, and excavated in 2010 by RAC, PJC plus E.  
538 Koppelhus, C. Coy (University of Alberta) and L. Martínez (Museo Argentino de Ciencias Naturales  
539 “Bernardino Rivadavia”). L. Garat (Universidad Nacional de Río Negro) found the referred specimen  
540 MLL-Pv-007. The specimens were prepared by E. Montes (Museo Carmen Funes, Plaza Huinca),  
541 photographed by S. Kagan (University of Alberta), and illustrated by RAC. Fieldwork and research was  
542 supported by CONICET Grants #0233, #0683 and UNRN-PI- 40-A-157, 297, 378 to RAC, whereas the  
543 expenses of PJC were supported by NSERC (Discovery Grant #203091-06) and the Dinosaur Research  
544 Institute (Calgary). We thanks the corrections and suggestions made from two anonymous reviewers and  
545 to Dr. Eduardo Koutsoukos, Editor-in-Chief of Cretaceous Research for his assistance and support.  
546 Finally, the authors are greatly indebted to the logistic support of the Municipality of Las Lajas, and  
547 particularly to the staff of the museum working under R. Faúndez with the support of P. Saldoval.

548

## 549 References

- 550 Allain, R., 2005. The postcranial anatomy of the megalosaur *Dubreuillosaurus valesdunensis* (Dinosauria  
551 Theropoda) from the middle Jurassic of Normandy, France *Journal of Vertebrate Paleontology* 25  
552 (4): 850–858.
- 553 Apesteguía, S., Smith, N.D., Juárez Valieri, R. and Makovicky, P.J., 2016. An unusual new theropod with  
554 a didactyl manus from the Upper Cretaceous of Patagonia, Argentina. *PloS one*, 11 (7):  
555 <https://doi.org/10.1371/journal.pone.0157793>
- 556 Britt, B. B., 1991. Theropods of Dry Mesa Quarry (Morrison Formation, Late Jurassic), Colorado, with  
557 emphasis on the osteology of *Torvosaurus tanneri*. *Brigham Young University Geology Studies*,  
558 37: 1-72.

- 559 Broom, R., 1904. On the occurrence of an opisthocoelian dinosaur (*Algoasaurus Bauri*) in the Cretaceous  
560 beds of South Africa. Geological Magazine, decade 5, 1 (483): 445-447.
- 561 Brusatte, S.L., Benson, R.B.J. and Hutt, S., 2008. The osteology of *Neovenator salerii* (Dinosauria:  
562 Theropoda) from the Wealden Group (Barremian) of the Isle of Wight. Palaeontographical  
563 Society Monograph 162: 1–75.
- 564 Brusatte, S.L., Benson, R.B., Chure, D.J., Xu, X., Sullivan, C. and Hone, D.W., 2009. The first definitive  
565 carcharodontosaurid (Dinosauria: Theropoda) from Asia and the delayed ascent of  
566 tyrannosaurids. Naturwissenschaften, 96 (9): 1051-1058.
- 567 Brusatte, S.L. and Sereno, P. C., 2007. A new species of *Carcharodontosaurus* (Dinosauria: Theropoda)  
568 from the Cenomanian of Niger and a revision of the genus. Journal of Vertebrate Paleontology,  
569 27 (4): 902-916.
- 570 Buffetaut, E., Cuny, G., Le Loeuff, J. and Suteethorn, V., 2009a. Late Palaeozoic and Mesozoic  
571 continental ecosystems of SE Asia: an introduction. Geological Society, London, Special  
572 Publications, 315 (1): 1-5.
- 573 Buffetaut, E., Suteethorn, V. and Tong, H., 2009b. An early 'ostrich dinosaur'(Theropoda:  
574 Ornithomimosauria) from the Early Cretaceous Sao Khua Formation of NE Thailand. Geological  
575 Society, London, Special Publications, 315 (1): 229-243.
- 576 Calvo, J.O. and Coria, R.A., 2000. New specimen of *Giganotosaurus carolinii* (Coria & Salgado, 1995),  
577 supports it as the largest theropod ever found. Gaia, 15: 117-122.
- 578 Calvo, J.O., Porfiri, J.D., Veralli, C., Novas, F. and Poblete, F., 2004. Phylogenetic status of *Megaraptor*  
579 *namunhuaiquii* Novas based on a new specimen from Neuquén, Patagonia, Argentina.  
580 Ameghiniana, 41 (4): 565-575.

- 581 Canale, J.I., Apesteguía, S., Gallina, P.A., Gianechini, F.A., and Haluza, A., 2017. The oldest theropods  
582 from the Neuquen Basin: Predatory dinosaur diversity from the Bajada Colorada Formation  
583 (Lower Cretaceous: Berriasian-Valanginian), Neuquen, Argentina. *Cretaceous Research* 71: 63-  
584 78.
- 585 Carpenter, K. and Ishida, Y., 2010. Early and “Middle” Cretaceous iguanodonts in time and space.  
586 *Journal of Iberian Geology*, 36 (2): 145-164.
- 587 Carrano, M.T., Benson, R.B.J., and Sampson, S.D., 2012. The phylogeny of Tetanurae (Dinosauria:  
588 Theropoda). *Journal of Systematic Palaeontology* 10: 211–300.
- 589 Cau, A., Dalla Vecchia, F.M. and Fabbri, M., 2013. A thick-skulled theropod (Dinosauria, Saurichia)  
590 from the Upper Cretaceous of Morocco with implications for caercharodontosaurid cranial  
591 evolution. *Cretaceous Research* 40: 251-260.
- 592 Chokchaloemwong, D., Hattori, S., Cuesta, E., Jintasakul, P., Shibata, M., Azuma, Y., 2019. A new  
593 carcharodontosaurid theropod (Dinosauria: Ornithischia) from the Lower Cretaceous of Thailand.  
594 *PloS ONE* 14 (10): e0222489. <https://doi.org/10.1371/journal.pone.0222489>
- 595 Christiansen, P. and Bonde, N., 2003. The first dinosaur from Denmark. *Neues Jahrbuch für Geologie*  
596 *und Paläontologie-Abhandlungen*, 287-299.
- 597 Coria, R. A., 2016. An overview of the ornithischian dinosaurs from Argentina. *Contribuciones del*  
598 *MACN* 6: 109-117.
- 599 Coria, R.A. and Currie, P.J., 2006. A new carcharodontosaurid (Dinosauria: Theropoda) from the Upper  
600 Cretaceous of Argentina. *Geodiversitas*. 28 (1):71-118.118.

- 601 Coria, R.A. and Currie, P.J., 2016. A new megaraptoran dinosaur (Dinosauria, Theropoda,  
602 Megaraptoridae) from the Late Cretaceous of Patagonia. PloS one, 11(7): e0157973.  
603 doi:10.1371/journal.pone.0157973
- 604 Coria, R., Currie, P.J., Koppelhus, E.B, Braun, A. and Cerda, I., 2010. First record of a Valanginian  
605 (Early Cretaceous) dinosaur association from South America. Journal of Vertebrate Paleontology  
606 30: 75A.
- 607 Coria, R. A., Currie, P., Ortega, F. and Baiano, M. A, 2017. A possible  
608 carcharodontosaurid theropod record from the Valanginian (Early Cretaceous) of Patagonia,  
609 Argentina. 77<sup>th</sup> Annual Meeting of the Society of Vertebrate Paleontology, Program and  
610 Abstracts: 100.
- 611 Coria, R.A., Ortega, F., Succar, C., Currie, P. and Koppelhus, E., 2012. First record of a dicraeosaurid  
612 sauropod from the Lower Cretaceous (Valanginian) of Neuquén Basin. XXVI Jornadas  
613 Argentinas de Paleontología de Vertebrados. Ameghiniana, 49 (Sup.4): R44.
- 614 Coria, R.A. and Salgado, L., 1995. A new giant carnivorous dinosaur from the Cretaceous of Patagonia.  
615 Nature, 377 (6546): 224-226.
- 616 Coria, R.A. and Salgado, L., 2005. Mid-Cretaceous turn-over of saurischian dinosaur communities:  
617 evidence from the Neuquén Basin. In Veiga, G. D., Spalletti, L. A., Howell, J.A. and Schwarz, E.  
618 (eds.) 2005. The Neuquén Basin, Argentina: A Case Study in Sequence Stratigraphy and Basin  
619 Dynamics. Geological Society, London, Special Publications, 252: 317–327.
- 620 Coria, R. A., Windholz, G. J., Ortega, F., and Currie, P. J., 2019. A new dicraeosaurid sauropod from the  
621 Lower Cretaceous (Mulichinco Formation, Valanginian, Neuquén Basin) of Argentina.  
622 Cretaceous Research, 93: 33-48.

- 623 Currie, P. J., 1995. New information on the anatomy and relationships of *Dromaeosaurus albertensis*  
624 (Dinosauria: Theropoda). *Journal of vertebrate Paleontology*, 15 (3): 576-591.
- 625 Currie, P.J. and Carpenter, K., 2000. A new specimen of *Acrocanthosaurus atokensis* (Theropoda,  
626 Dinosauria) from the lower Cretaceous Antlers Formation (Lower Cretaceous, Aptian) of  
627 Oklahoma, USA. *Geodiversitas*, 22 (2): 207-246.
- 628 Currie, P.J. and Chen, P.J., 2001. Anatomy of *Sinosauropteryx prima* from Liaoning, northeastern China.  
629 *Canadian Journal of Earth Sciences*, 38 (12): 1705-1727.
- 630 Currie, P.J. and Zhao, X., 1993. A new carnosaur (Dinosauria, Theropoda) from the Upper Jurassic of  
631 Xinjiang, People's Republic of China. *Canadian Journal of Earth Sciences* 30 (10): 2037-2081.  
632 doi:10.1139/e93-179.
- 633 de Azevedo, R.P.F., Simbras, F.M., Furtado, M.R., Candeiro, C.R.A., and Bergqvist, L.P., 2013. First  
634 Brazilian carcharodontosaurid and other new theropod dinosaur fossils from the Campanian–  
635 Maastrichtian Presidente Prudente Formation, São Paulo State, southeastern Brazil. *Cretaceous*  
636 *Research*, 40, 131-142.
- 637 de Klerk, W. J., Forster, C. A., Sampson, S. D., Chinsamy, A. and Ross, C. F., 2000. A new  
638 coelurosaurian dinosaur from the Early Cretaceous of South Africa. *Journal of Vertebrate*  
639 *Paleontology*, 20 (2): 324-332.
- 640 D'Emic, M., Melstrom, K. and Eddy, D., 2012. Paleobiology and geographic range of the large-bodied  
641 Cretaceous theropod dinosaur *Acrocanthosaurus atokensis*. *Palaeogeography, Palaeoclimatology,*  
642 *Palaeoecology*, 333: 13–23. 10.1016/j.palaeo.2012.03.003.
- 643 Eddy, D. R. and Clarke, J. A., 2011. New information on the cranial anatomy of *Acrocanthosaurus*  
644 *atokensis* and its implications for the phylogeny of Allosauroidea (Dinosauria: Theropoda). *PloS*  
645 *one*, 6(3): <https://doi.org/10.1371/journal.pone.0017932>

- 646 Ezcurra, M. D. and Novas, F. E., 2016. Theropod dinosaurs from Argentina. *Historia Evolutiva y*  
647 *Paleobiogeográfica de los Vertebrados de América del Sur. Contribuciones del MACN*, 6: 139-  
648 56.
- 649 França, M.A.G., Ferigolo, J. and Langer, M.C., 2011. Associated skeletons of a new middle Triassic  
650 “Rauisuchia” from Brazil. *Naturwissenschaften*, 98 (5): 389-395.
- 651 Galton, P.M., 2009. Notes on Neocomian (Lower Cretaceous) ornithopod dinosaurs from England -  
652 *Hypsilophodon, Valdosaurus, “Camptosaurus”, “Iguanodon”* - and referred specimens from  
653 Romania and elsewhere. *Revue de Paléobiologie*, 28 (1): 211-273
- 654 Gallina, P.A., Apesteguía, S., Haluza, A., Canale, J.I., 2014. A diplodocid sauropod  
655 survivor from the Early Cretaceous of South America. *PLoS ONE* 9 (5): e97128.  
656 doi:10.1371/journal.pone.0097128
- 657 Gallina, P. A., Apesteguía, S., Canale, J. I., and Haluza, A., 2019. A new long-spined  
658 dinosaur from Patagonia sheds light on sauropod defense system. *Scientific reports*, 9 (1):1392.
- 659 Gauthier, J. 1986. Saurischian monophyly and the origin of birds. *Memoirs*  
660 *of the Californian Academy of Science* 8:1-55.
- 661 Gerke, O., and Wings, O., 2016, Multivariate and cladistic analyses of isolated teeth  
662 reveal sympatry of theropod dinosaurs in the Late Jurassic of Northern Germany: *PLoS ONE*, v.  
663 11, doi:10.1371/journal.pone.0158334
- 664 Gilmore, C.W., 1920. *Osteology of the carnivorous Dinosauria in the United States*  
665 *National museum: with special reference to the genera Antrodemus (Allosaurus) and*  
666 *Ceratosaurus* (No. 110). US Government printing office, pp. 1-159.



- 667 Goloboff, P. and Catalano, S., 2016. TNT, version 1.5, with a full implementation of phylogenetic  
668 morphometrics. *Cladistics*, doi:10.1111/cla. 12160
- 669 Gnaedinger, S., Coria, R.A., Koppelhus, E., Casadío, S., Tunik, M. and Currie, P., 2017. First Lower  
670 Cretaceous record of Podocarpaceae wood associated with dinosaur remains from Patagonia,  
671 Neuquén Province, Argentina. *Cretaceous Research*, 78: 228-239.
- 672 Gulisano, C.A., Gutierrez Pleimling, A.R. and Digregorio, R.E., 1984. Análisis estratigráfico del  
673 intervalo Tithoniano-Valanginiano (formaciones Vaca Muerta, Quintuco y Mulichinco) en el  
674 suroeste de la provincia del Neuquén. IX Congreso Geológico Argentino, Actas I: 221-235.
- 675 Han, F., Clark, J.M., Xu, X., Sullivan, C., Choiniere, J., and Hone, D.W.E., 2011, Theropod teeth from  
676 the Middle-Upper Jurassic Shishugou Formation of northwest Xinjiang, China: *Journal of*  
677 *Vertebrate Paleontology*, v. 31: 111–126.
- 678 Harris, J.D., 1998. A reanalysis of *Acrocanthosaurus atokensis*, its phylogenetic status, and  
679 paleobiogeographic implications, based on a new specimen from Texas: *Bulletin 13 (Vol. 13).*  
680 *New Mexico Museum of Natural History and Science.*
- 681 Harrison, C. J. O. and Walker, C. A., 1973. *Wyleyia*: a new bird humerus from the Lower Cretaceous of  
682 England. *Palaeontology*, 16 (Part 4): 721-728.
- 683 Janensch, W., 1914. Übersicht über die Wirbeltierfauna der Tendaguruschichten, nebst  
684 einer kurzen Charakterisierung der neu aufgeführten Arten von Sauropoden. *Archiv für*  
685 *Biontologie* 3 (1): 81-110.
- 686 Lamanna, M. C., Martínez, R. D. and Smith, J. B., 2002. A definitive abelisaurid theropod dinosaur from  
687 the early Late Cretaceous of Patagonia. *Journal of Vertebrate Paleontology*, 22(1): 58-69.

- 688 Madsen, J. H., 1976. *Allosaurus fragilis*: a revised osteology. Utah Geological and Mining Survey  
689 Bulletin, 109: 1-163.
- 690 Madsen, J. H. and Welles, S. P., 2000. *Ceratosaurus* (Dinosauria, Theropoda): a revised osteology. Utah  
691 Geological Survey, pp. 80.
- 692 Malafaia, E., Mocho, P., Escaso, F., and Ortega, F., 2017. A juvenile allosauroid theropod (Dinosauria,  
693 Saurischia) from the Upper Jurassic of Portugal. *Historical Biology*, 29 (5): 654-676. DOI:  
694 10.1080/08912963.2016.1231183
- 695 Malafaia, E., Mocho, P., Escaso, F. and Ortega, F. 2019. Carcharodontosaurian Remains (Dinosauria,  
696 Theropoda) from the Upper Jurassic of Portugal. *Journal of Paleontology* 93(1): 157–172.
- 697 Marsh, O.C., 1881. Principal characters of American Jurassic dinosaurs.  
698 Part V. *American Journal of Science*, series 3 (21):417–423.
- 699 Martínez, L.C.A., Olivo, M., Koppelhus, E. and Coria, R.A., 2012. First record of *Tempskya* Corda from  
700 Mulichinco Formation (Valanginian), Sierra De La Vaca Muerta, Neuquén Basin, Argentina.  
701 Ameghiniana. XV Simposio Argentino de Paleobotánica y Palinología. Expositor. 10 al 13 de  
702 julio de 2012. Corrientes. Argentina, 49 (Sup.4): R117.
- 703 Motta, M.J., Aranciaga Rolando, A.M., Rozadilla, S., Agnolín, F.E., Chimento, N.R., Egli, F.B. and  
704 Novas, F.E., 2016. New theropod fauna from the Upper Cretaceous (Huincul Formation) of  
705 Northwestern Patagonia, Argentina. *New Mexico Museum of Natural History and Science*  
706 Bulletin 71: 231-253.
- 707 Norman, D. B., 2010. A taxonomy of iguanodontians (Dinosauria: Ornithopoda) from the lower Wealden  
708 Group (Cretaceous: Valanginian) of southern England. *Zootaxa*, 2489: 47-66.

- 709 Norman, D. B., 2012. Iguanodontian taxa (Dinosauria: Ornithischia) from the Lower Cretaceous of  
710 England and Belgium. In P. Godefroit (Ed.), *Bernissart Dinosaurs, and Early Cretaceous*  
711 *terrestrial ecosystem*, Indiana University Press, Bloomington, pp. 175-212.
- 712 Novas, F.E., de Valais, S., Vickers-Rich, P. and Rich, T., 2005. A large Cretaceous theropod from  
713 Patagonia, Argentina, and the evolution of carcharodontosaurids. *Naturwissenschaften*, 92(5):  
714 226-230.
- 715 Ortega, F., Escaso, F. and Sanz, J.L., 2010. A bizarre, humped Carcharodontosauria (Theropoda) from the  
716 Lower Cretaceous of Spain. *Nature*, 467 (7312), 203-205.
- 717 Paulina Carabajal, A., Coria, R.A., Currie, P.J. and Koppelhus, E.B., 2018. A natural  
718 cranial endocast with possible dicraeosaurid (Sauropoda, Diplodocoidea) affinities from the  
719 Lower Cretaceous of Patagonia. *Cretaceous Research* 84: 437-441.
- 720 Pereda-Suberbiola, X., Ruiz-Omeñaca, J. I., Canudo, J. I., Torcida, F. and Sanz, J. L.,  
721 2012. Dinosaur faunas from the Early Cretaceous (Valanginian-Albian) of Spain. In P. Godefroit  
722 (Ed.), *Bernissart dinosaurs and Early Cretaceous terrestrial ecosystem*. Indiana University Press,  
723 Bloomington, 379-407.
- 724 Rauhut, O.W.M., 2011. Theropod dinosaurs from the Late Jurassic of Tendaguru (Tanzania).  
725 *Palaeontology, Special Papers in Palaeontology*, 86: 195–239.
- 726 Rauhut, O. W. and Xu, X., 2005. The small theropod dinosaurs *Tugulusaurus* and *Phaedrolosaurus* from  
727 the Early Cretaceous of Xinjiang, China. *Journal of Vertebrate Paleontology*, 25(1): 107-118.
- 728 Remes, K., 2004. Der Tendaguru-Sauropode “*Barosaurus*” africanus und die Palaobiogeographie der  
729 Diplodocidae (Sauropoda). *Geobiologie*, 74, 195-196.

- 730 Salgado, L. and Calvo, J.O., 2016. La contribución argentina al conocimiento de los dinosaurios  
731 saurópodos: 1984-2016. *Contribuciones del MACN*, 6: 129-137.
- 732 Sampson, S. D. and Witmer, L. M., 2007. Craniofacial anatomy of *Majungasaurus crenatissimus*  
733 (Theropoda: Abelisauridae) from the late Cretaceous of Madagascar. *Journal of Vertebrate*  
734 *Paleontology*, 27(S2): 32-104.
- 735 Sereno, P.C., and Brusatte, S.L., 2008. Basal abelisaurid and carcharodontosaurid theropods from the  
736 Lower Cretaceous Elrhaz Formation of Niger. *Acta Palaeontologica Polonica* 53: 15–46.
- 737 Sereno, P.C., Dutheil, D.B., Iarochene, M. and Larsson, H.C., 1996. Predatory dinosaurs from the Sahara  
738 and Late Cretaceous faunal differentiation. *Science*, 272(5264): 986.
- 739 Sereno, P.C., Martinez, R.N., Wilson, J.A., Varricchio, D.J., Alcober, O.A. and Larsson, H.C., 2008.  
740 Evidence for avian intrathoracic air sacs in a new predatory dinosaur from Argentina. *PLoS One*,  
741 3 (9), e3303.
- 742 Stovall, J.W. and Langston, W., 1950. *Acrocanthosaurus atokensis*, a new genus and species of Lower  
743 Cretaceous Theropoda from Oklahoma. *The American Midland Naturalist*, 43(3): 696-728.
- 744 Stromer, E., 1931. Wirbeltierreste der Baharije-Stufe (unterstes Cenoman). 10. Ein Skelett-Rest von  
745 *Carcharodontosaurus* nov. gen. *Abhandlungen Bayerische Akademie Wissenschafte Atheilung-*  
746 *naturwissenschaften Abteilung Neue Folge*, 9: 1–23.
- 747 Taylor, M. P. and Naish, D., 2007. An unusual new neosauropod dinosaur from the Lower Cretaceous  
748 Hastings Beds Group of East Sussex, England. *Palaeontology*, 50 (6): 1547-1564.
- 749 Weishampel, D.B., Barrett, P.M., Coria, R.A., Le Loeuff, J., Xing, X., Xijin, Z., Sahni, A., Gomani,  
750 E.M.P. and Noto, C.R., 2004. Dinosaur distribution. In *The Dinosauria*, Second Edition,  
751 University of California Press, Berkeley, Los Angeles, London, pp. 517-606.

- 752 You, H., Ji, Q., and Li, D., 2005. *Lanzhousaurus magnidens* gen. et sp. nov. from Gansu Province, China:  
753 the largest-toothed herbivorous dinosaur in the world. *Geological Bulletin of China*, 24 (9): 785-  
754 794.
- 755 Zanno, L. and Makovicky, P.J., 2013. Neovenatorid theropods are apex predators in the Late Cretaceous  
756 of North America. *Nature Communications* 4: 2827, doi:10.1038/ncomms3827.
- 757 Zavala, C., 1999. Análisis estratigráfico de la Formación Mulichinco (Valanginiano) en el centro-oeste de  
758 la Cuenca Neuquina, Provincia del Neuquén. XIV Congreso Geológico Argentino. *Actas* 1: 77.
- 759 Zavala, C., 2000. Nuevos avances en la sedimentología y estratigrafía secuencial de la Formación  
760 Mulichinco (Valanginiano) en la Cuenca Neuquina. *Boletín de Informaciones Petroleras*. Tercera  
761 Época, año XVII, N° 63: 40-54.
- 762 Zavala, C.A., Mosquera, A. and Kim, H.J., 2005. Los depósitos eólicos de la Formación Mulichinco. VI  
763 Congreso de Exploración y Desarrollo de Hidrocarburos. *Actas Cdrom*, 14 pp. Mar del Plata.

764

765

**766 FIGURE CAPTIONS**

767

768 Figure 1. Restoration of *Lajasvenator ascheriae* showing which bones have been collected.

769

770 Figure 2. Location map showing provenance of specimens MLL-PV-005 and MLL-PV-007 (after Coria et  
771 al., 2019). Quarries indicated by the arrow.

772

773 Figure 3. Stratigraphical section and geological provenance of *Lajasvenator ascheriae* remains (modified  
774 from Coria et al., 2019).

775

776 Figure 4. *Lajasvenator ascheriae*, Holotype, MLL-PV-005. Premaxillae and maxilla in A) left lateral, B)  
777 right lateral, C) anterior and D) ventral views. Abbreviations: mx, maxilla; pmx, premaxilla; snp,  
778 supranarial process; v, vomers. Scale bar: 10 cm.

779

780 Figure 05. *Lajasvenator ascheriae*, MLL-Pv-007. Right quadratojugal in A) posterior, B) lateral, and C)  
781 medial views. Abbreviations: ljs, suture for lower prong of jugal; qf, limits of border of quadratic fenestra  
782 formed by quadratojugal; qs, quadrate suture; ujs, range of suture of upper prong of jugal. Scale bar: 10  
783 cm.

784

785 Figure 6. *Lajasvenator ascheriae*, MLL-Pv-007. Anterior ends of dentaries. Left dentary in A) lateral and  
786 D) medial views; right dentary in B) lateral, C) dorsal and E) medial views. Tooth crowns seen on the  
787 right side in dt2 and dt3, whereas broken roots are visible in dt1 and dt4. On the left side, part of the crown  
788 is visible in dt1, and broken roots can be seen in dt2 and dt3. Abbreviations: ch, chin-like process; dt1 to  
789 dt4, dentary tooth positions; id, interdental plate; mg, Meckelian groove. Scale bar: 5 cm.

790

791 Figure 7. *Lajasvenator ascheriae*, Holotype, MLL-Pv-005. Left dentary in lateral view. Abbreviation: mf,  
792 mandibular fenestra. Scale bar: 10 cm.

793

794 Figure 8. *Lajasvenator ascheriae*, Holotype, MLL-Pv-005. Left splenial in medial view. Abbreviation: aa,  
795 articulation for the angular. Scale bar: 10 cm.

796

797 Figure 9. *Lajasvenator ascheriae*, Holotype, MLL-Pv-005. Last four cervical vertebrae, first dorsal  
798 vertebra, and ribs in articulation as found in left lateral view. Abbreviations: 6<sup>th</sup> to 10<sup>th</sup>, sixth to tenth  
799 cervical vertebrae; r5<sup>th</sup> to r10<sup>th</sup>, fifth to tenth cervical ribs. Scale bar: 10 cm.

800

801 Figure 10. *Lajasvenator ascheriae*, Holotype, MLL-Pv-005. Sixth cervical vertebra in A) left lateral, B)  
802 anterior, C) posterior, and D) ventral views. Abbreviations: c, anterior articular surface of centrum; pp,  
803 parapophysis. Scale bar: 10 cm.

804

805 Figure 11. *Lajasvenator ascheriae*, Holotype, MLL-Pv-005. Seventh cervical vertebra in A-A') left  
806 lateral, B-B') anterior, C-C') posterior, D-D') dorsal, and E-E') ventral views. A-E, photographs; A'-E',  
807 line drawings. Abbreviations: dp, diapophysis; ep, epipophysis; ns, neural spine; pl, pleurocoel; prz,  
808 prezygapophysis; pz, postzygapophysis. Scale bar: 10 cm.

809

810 Figure 12. *Lajasvenator ascheriae*, Holotype, MLL-Pv-005. Eighth cervical vertebra in A-A') left lateral,  
811 B-B') anterior, C-C') posterior, E-E') dorsal, and D-D') ventral views. A-D, photographs; A'-D', line  
812 drawings. Abbreviations: as in Fig.11. Scale bar: 10 cm.

813

814 Figure 13. *Lajasvenator ascheriae*, Holotype, MLL-Pv-005. Ninth cervical vertebra in A-A') left lateral,  
815 B-B') anterior, C-C') posterior, E-E') dorsal, and D-D') ventral views. A-D, photographs; A'-D', line  
816 drawings. Abbreviations: as in Fig.11. Scale bar: 10 cm.

817

818

819 Figure 14. *Lajasvenator ascheriae*, Holotype, MLL-Pv-005. Tenth presacral vertebra (Dorsal 1) in A-A')  
820 left lateral, B-B') anterior, C-C') posterior, E-E') dorsal, and D-D') ventral views. A-D, photographs; A'-  
821 D', line drawings. Abbreviations: as in Fig.11. Scale bar: 10 cm.

822

823 Figure 15. *Lajasvenator ascheriae*, Holotype, MLL-Pv-005. Articulated series of dorsal centra in right  
824 ventrolateral view. Abbreviations: 15<sup>th</sup>, fifteenth presacral vertebra; 23<sup>th</sup>, twentyeighth presacral vertebra;  
825 dp, diapophysis. Scale bar: 10 cm.

826

827 Figure 16. *Lajasvenator ascheriae*, Holotype, MLL-Pv-005. Mid-caudal vertebrae in A) lateral, and B)  
828 ventral views. Abbreviations: c, vertebral centrum; prz, prezygapophysis; ns, neural spine; sp, spinous  
829 process; tp, transverse process. Scale bar: 10 cm.

830

831 Figure 17. *Lajasvenator ascheriae*, Holotype, MLL-Pv-005. Left cervical ribs in lateral view.

832 Abbreviations: 6cr-9cr, sixth to ninth cervical rib; bap, bilobed anterior process. Scale bar: 10 cm.

833



834 Figure 18. *Lajasvenator ascheriae*, Holotype, MLL-Pv-005. Left dorsal ribs in lateral view.

835 Abbreviations: 8dr-13dr, eighth to thirteenth dorsal rib. Scale bar: 10 cm.

836

837 Figure 19. *Lajasvenator ascheriae*, Holotype, MLL-Pv-005. Pelvic elements in A) right lateral and B)

838 right medial views. Abbreviations: ib, iliac blade; is, ischium; p, pubis; pa, pubic apron; ppc, pubic

839 pedicel; prp; preacetabular process; sr, sacral rib. Scale bar: 10 cm.

840

841 Figure 20. *Lajasvenator ascheriae*, Holotype, MLL-Pv-005. Ilium and pubis articulation in A) right

842 lateral, B) posterior, and C) right medial views. Abbreviations: ac, acetabulum; il, ilium; is, ischium; pa;

843 pubic apron. Scale bar: 10 cm.

844

845 Fig. 21. *Lajasvenator ascheriae*, MLL-Pv-007. Possible carpal/tarsal in A) dorsal, B) ventral; C) anterior,

846 and D) posterior views. Scale bar: 1 cm.

847

848 Fig. 22. Simplified cladogram depicting the phylogenetic relationships of *Lajasvenator ascheriae* within

849 Carcharodontosauridae.

850

851

852

853

Tooth	DHmin	CHJM	CHPC	FABL	AntDent	PostDent	BW	BW/FABL	AL	AW	AW/AL
Pmx 1 R	?	?	?	?	?	?	?	?	9.1	7.1	0.78
Pmx 1 L	?	?	?	?	?	?	?	?	9.2	6.5	0.71
Pmx 2 L	?	?	?	?	?	?	?	?	11.4	5.7	0.50
Pmx 3 R	?	25.7	20.9	10.1	2.7	3	6.2	0.61	12	7.1	0.59
Pmx 4 R	?	10.2	?	5.8	?	?	4.7	0.81	10.3	6.1	0.59
Pmx 4 L	?	25plus	?	8.5	?	?	6.4	0.75	?	?	?
Mx 1 L	?	?	?	?	?	?	?	?	10.7	4.8	0.45
Mx 2 L	?	?	?	?	?	?	?	?	13.4	6	0.45
Mx 3 R	?	?	?	?	?	?	?	?	15.6	6	0.38
Mx 3 L	?	?	?	?	?	?	?	?	16.8	6.4	0.38
Mx 4 R	?	?	?	?	?	?	?	?	13plus	?	?
Mx 4 L	?	?	?	?	?	?	?	?	17.1	7.2	0.42
Mx 5 L	?	?	?	?	?	?	?	?	20.8	8.1	0.39
Mx 6 L	?	?	?	?	?	?	?	?	18.3	7.4	0.40
Mx 7 L	?	?	?	?	?	?	?	?	10plus	?	?
D 1 R	53.2	?	?	?	?	?	?	?	?	5.1	?
D 1 L	53.2	?	?	?	?	?	?	?	8.1	4.3	0.40
D 2 R	53.2	13plus	?	14.2	?	?	6.4	0.45	14.5	7.1	0.49
D 2 L	53.2	?	?	?	?	?	?	?	11.7	?	?
D 3 R	53.2	?	?	?	?	?	?	?	14.7	6.8	0.46
D 3 L	53.2	?	?	?	?	?	?	?	14.3	6.1	0.40
D 4 R	53.2	?	?	?	?	?	?	?	?	5.1plus	?
D 4 L	53.2	?	?	?	?	?	?	?	?	6plus	?
D 4 L	53,2	?	?	?	?	?	?	?	?	6plus	?

Table 1. Teeth and alveoli measurements of *Lajasvenator ascherieae*. Premaxillary and maxillary teeth from specimen MLL-Pv-005, Holotype; dentary teeth from specimen MLL-Pv-007. Abbreviations: ?, unknown; AL, anteroposterior length of alveolus; AW, transverse alveolus width; AntDent, number of anterior denticles per mm; BW, basal width of crown; D, dentary tooth; DHmin, minimum height of dentary; CHJM, crown height from the jaw margin, CHPC, crown height along posterior carina; FABL, fore-aft basal length; L, left; Mx, maxillary tooth; Pmx, premaxillary tooth; PostDent, number of posterior denticles per mm; R, right. All measurements in mm.

	clnas	clv	clwc	caww	cah	cpw	cph	cnw	th	nsh	nmdl	wap	wapz	llppz	watp	wapp
<b>6</b>	82	81	102	57	64	61.5	59.8	29	?	?	?	?	83est	?	?	60.6
<b>7</b>	66.8	72	90	63	36	62.3	47.8	30.5	126.5	66.5	29	74	71.6	109.6	128	66
<b>8</b>	65	69.5	103	48	43	65	47	32.1	129	68	30	68.8	69	86.4	134	71.3
<b>9</b>	62	65.1	92	59	40.5	68.5	48.9	34.2	128.3	64.7	21	70	74	66	144.4	66.6
<b>10</b>	?	?	?	59.5	44plus	?	?	?	124plus	69.2	17	73.7	?	?	150	59.4
<b>15</b>	47plus	?	?	?	?	?	?	?	?	?	?	?	?	?	?	?
<b>16</b>	70.5	71	?	61.5	59est	60.6	58est	14.4	?	?	?	?	?	?	?	?
<b>17</b>	71.4	64.9	?	63.4	53plus	53.6	56.3	15.5	?	?	?	?	?	?	?	?
<b>18</b>	72.6	65.6	?	49	52.3	55	60.6	15.3	?	?	?	?	?	?	164est	?
<b>19</b>	?	?	?	?	?	?	86	?	?	?	?	?	?	?	160est	?
<b>20</b>	68	68.7	?	53plus	88.3	65.7	77.2	16plus	?	?	?	?	?	?	160est	?
<b>21</b>	74.2	70.1	?	70	82.3	70.5	79.4	25	?	?	?	?	?	?	156	49
<b>22</b>	71.3	67.5	?	75.6	80.4	66plus	83	27.1	?	?	?	?	?	?	124plus	54.3
<b>23</b>	?	?	?	?	93.6	?	?	27	?	?	?	?	?	?	?	?
<b>S2</b>	?	59plus	?	?	?	?	?	32	?	?	?	?	?	?	?	?
<b>S3</b>	?	68	?	55	?	58	?	35	?	?	?	?	?	?	89	?
<b>S4</b>	?	35plus	?	58	?	58	?	?	?	?	?	?	?	?	60est	?
<b>C15</b>	?	?	?	?	?	?	?	?	?	?	?	?	24.4	?	?	?
<b>C16</b>	?	?	?	?	?	?	?	?	?	?	?	?	?	?	?	?
<b>C16</b>	58plus	?	?	?	?	30.8	39.6	13	104	61	20.8	30.3	24.6	84	88est	?
<b>C17</b>	?	?	?	?	?	?	?	?	?	?	?	?	?	?	?	?
<b>C17</b>	65.5	66	?	31.6	34.7	33.6	41	14.2	99	58est	23	38	24.6	81	100	?
<b>C18</b>	?	?	?	?	?	?	?	?	?	?	?	?	?	?	?	?
<b>C18</b>	65.3	67	?	38.6	36	32.4	36	15.6	?	?	?	41	?	?	96.7	?

Table 2. *Lajasvenator ascherieae*, Holotype, specimen MLL-Pv-005. Table of vertebral measurements. Abbreviations; 6 to 23: presacral vertebrae 6<sup>th</sup> to 23<sup>rd</sup>; ?, unknown; C, caudal vertebrae; cah, centrum anterior height; caw, centrum anterior width; clnas, centrum length at neural arch suture; clv, centrum length at ventral side; clwc, centrum length with condyle; cnw, centrum narrowest width; cph, centrum posterior height; cpw, centrum posterior width; est, estimated; lppz, length prezygapophyseis – postzygapophysis; nmdl, neural spine maximum distal

length; nsh, neural spine height above canal roof; S, sacral vertebrae; th, total height; wap, width across prezygapophyseis; wapp, width across parapophyses; wapz, width across postzygapophyses; watp, width across transverse processes. All measurements in mm.

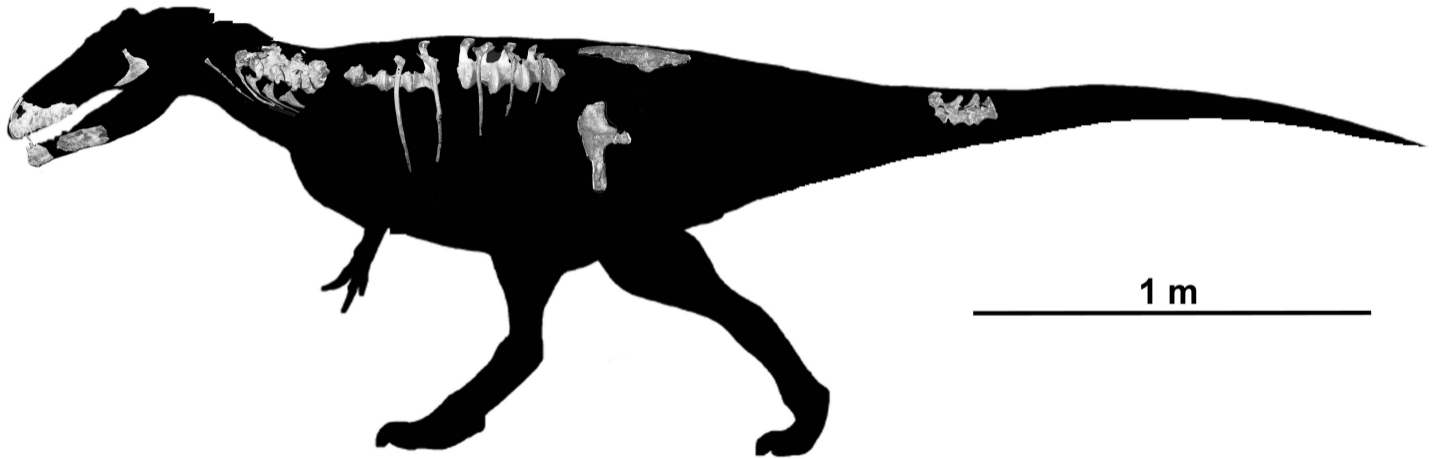
Journal Pre-proof

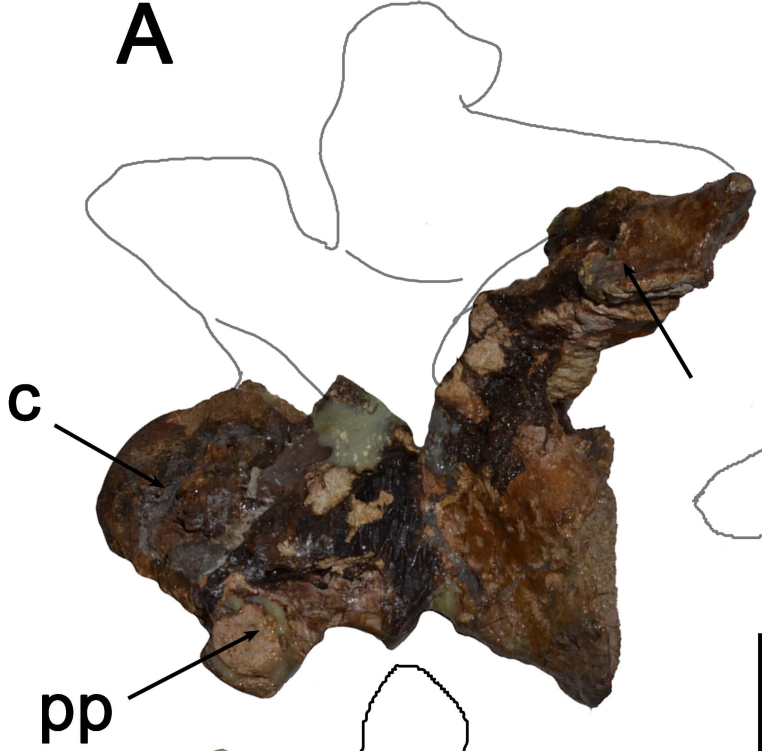
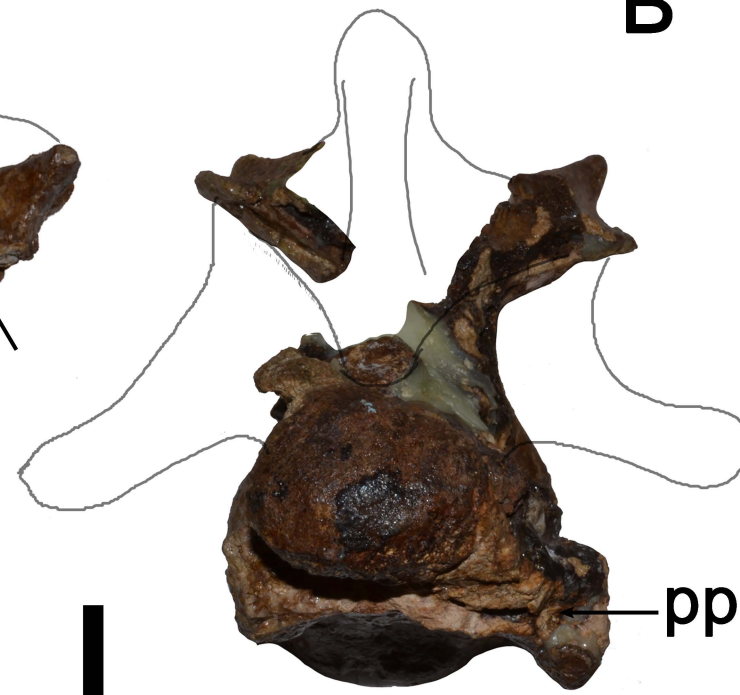
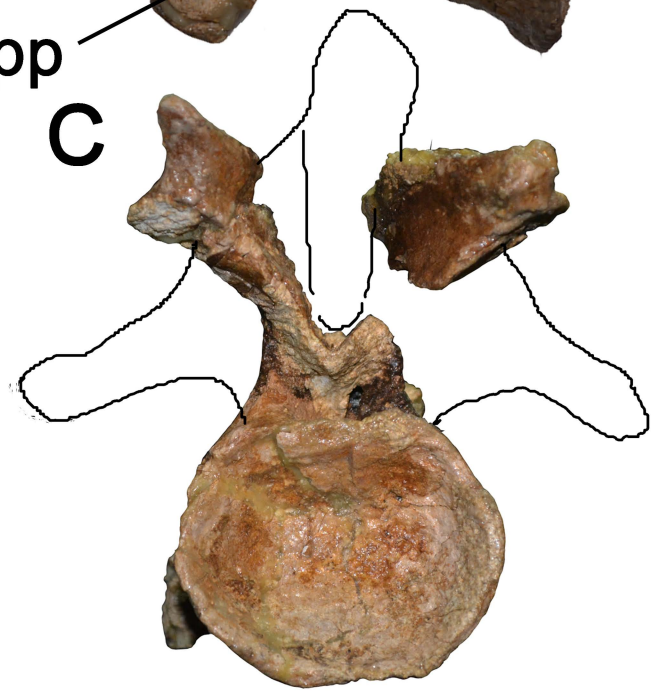
A new genus and species of carcharodontosaurid theropod (*Lajasvenator ascheriae*) is described.

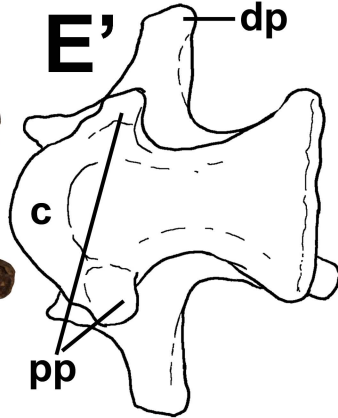
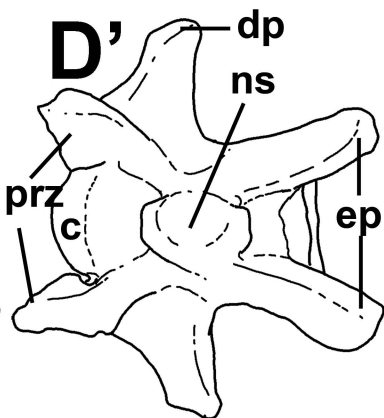
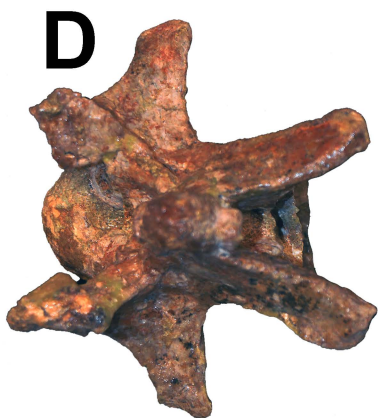
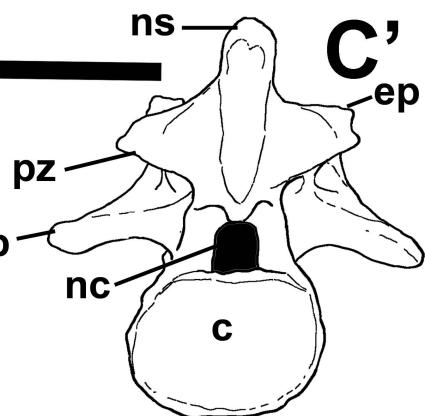
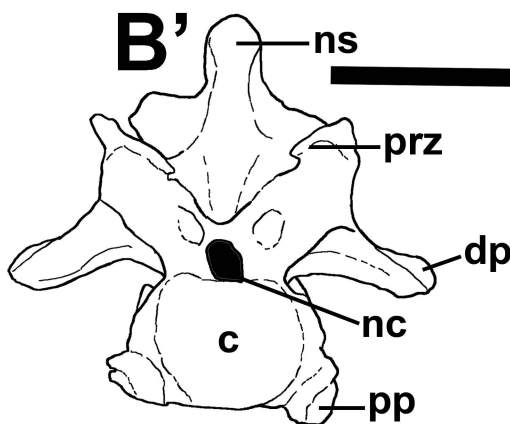
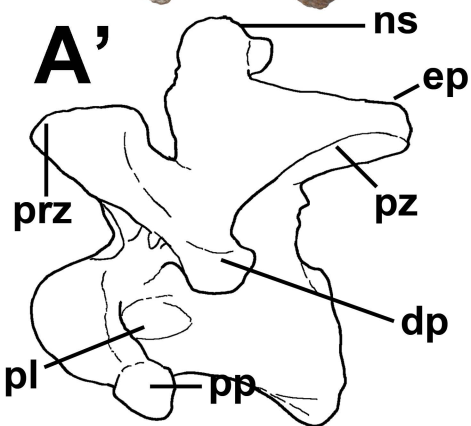
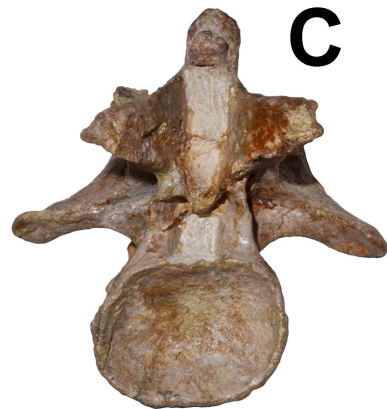
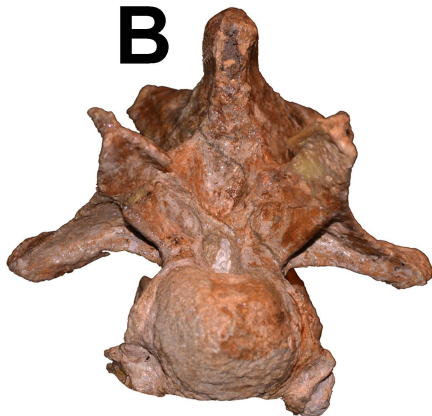
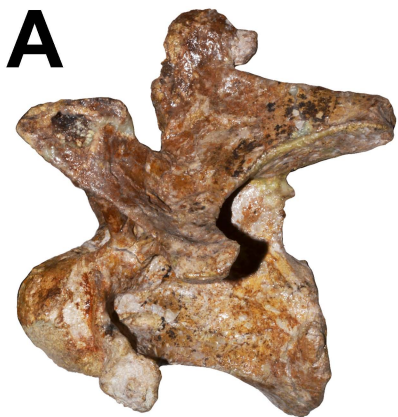
*Lajasvenator* is the oldest Cretaceous carcharodontosaurid record.

*Lajasvenator* represents the first Lower Cretaceous, South American carcharodontosaurid.

Journal Pre-proof

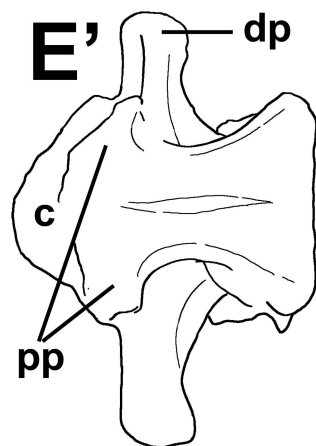
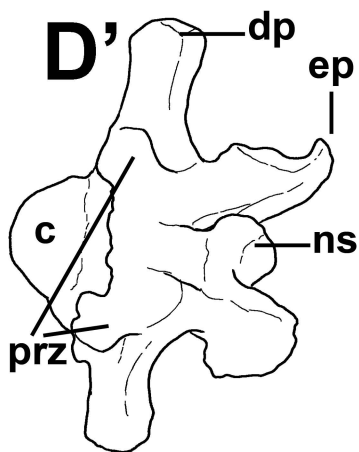
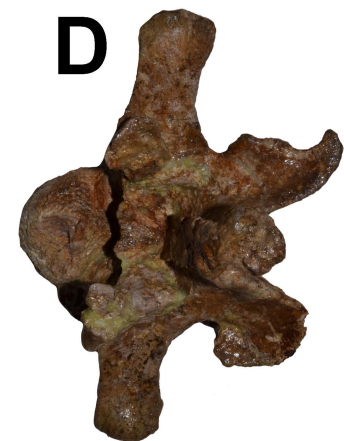
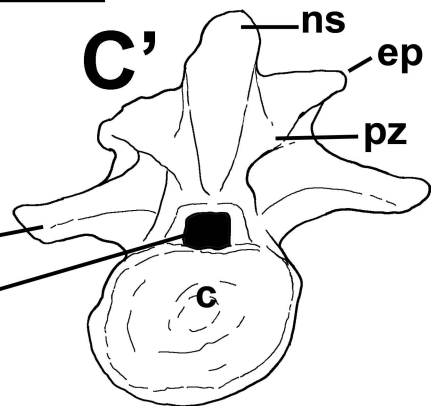
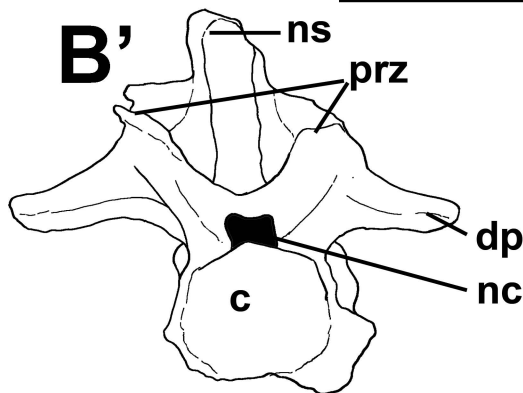
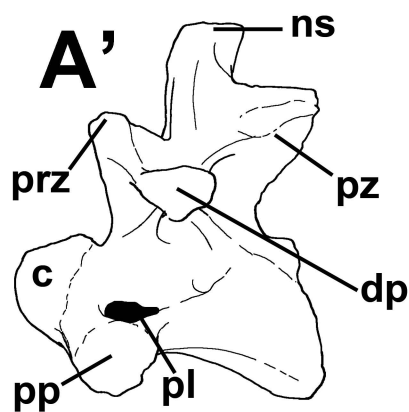
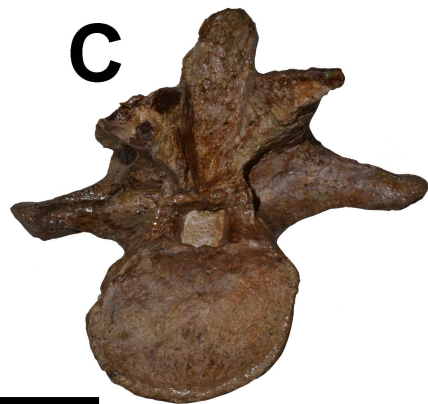
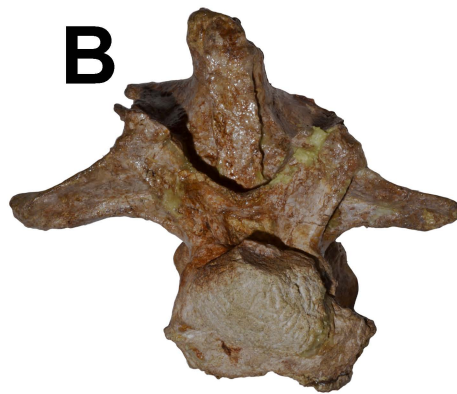
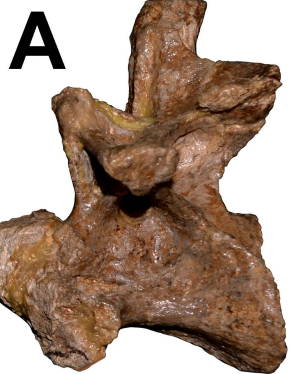


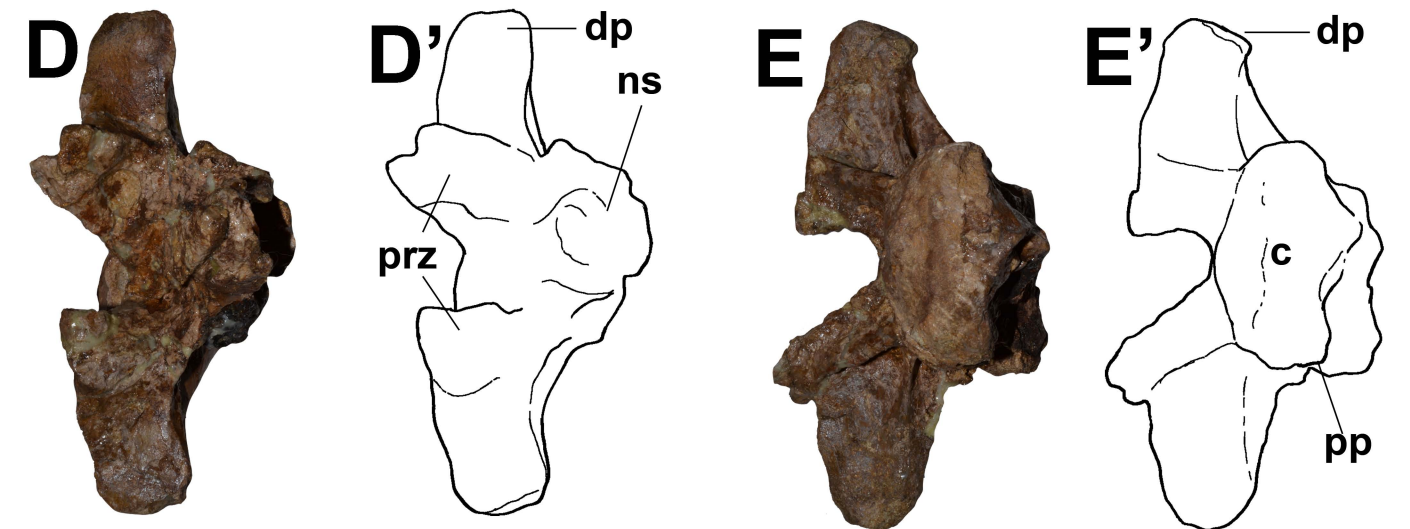
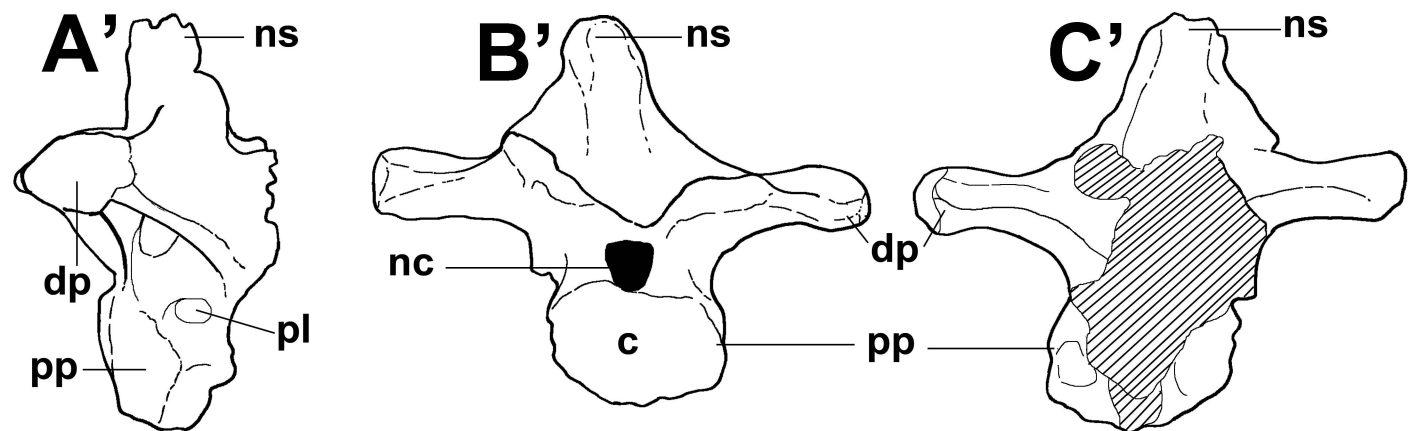
**A****B****C****D**

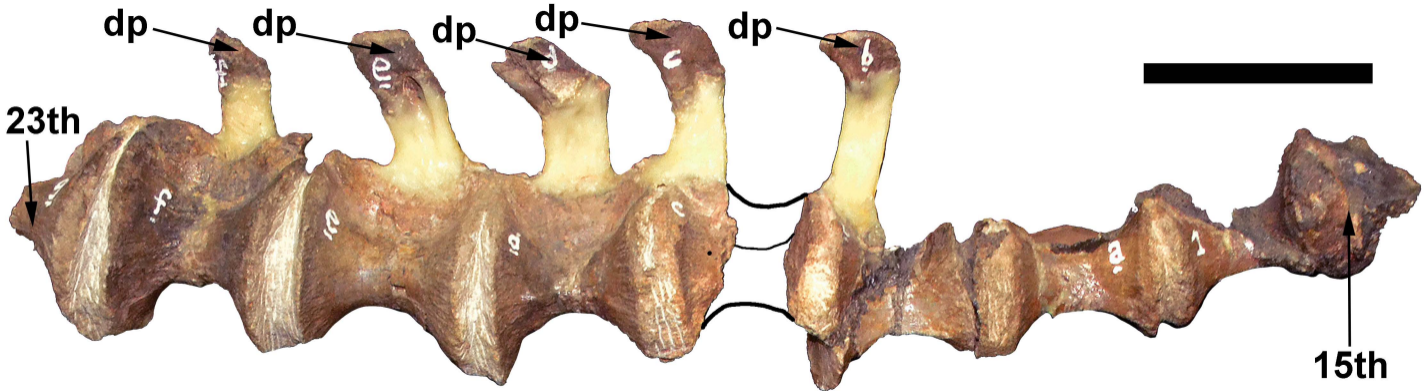


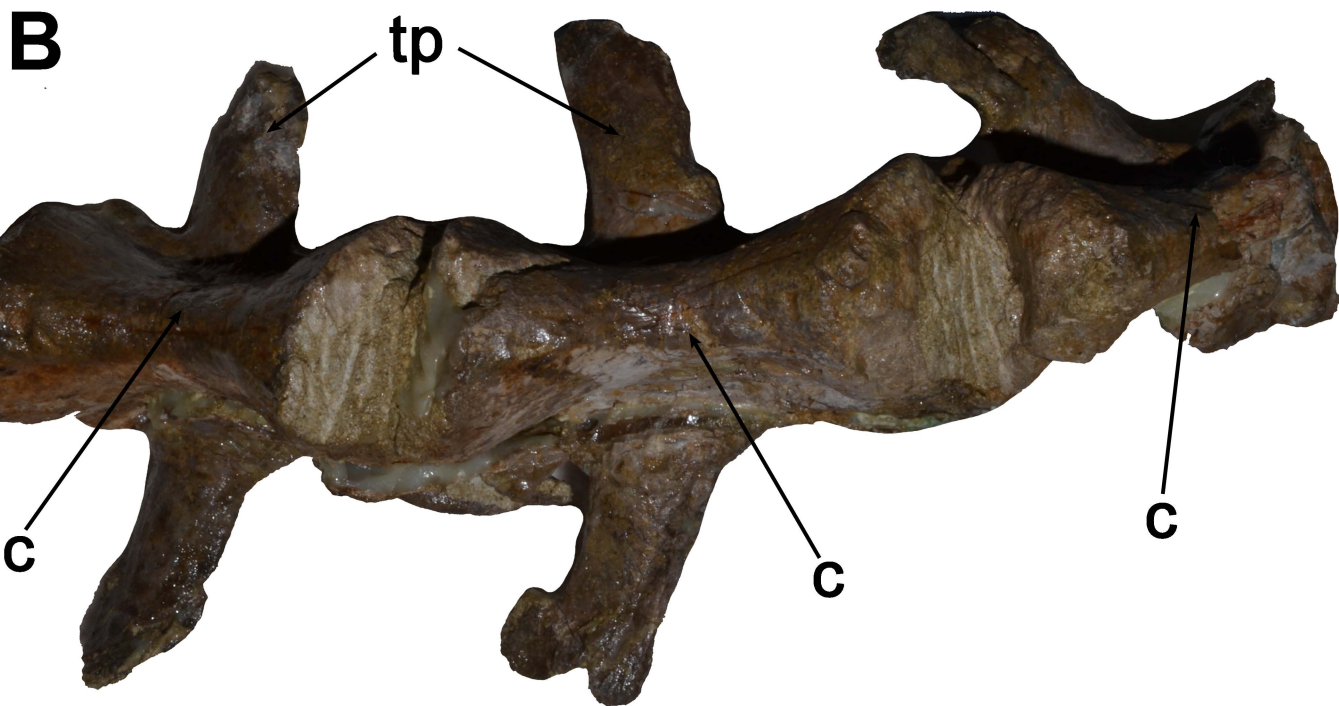
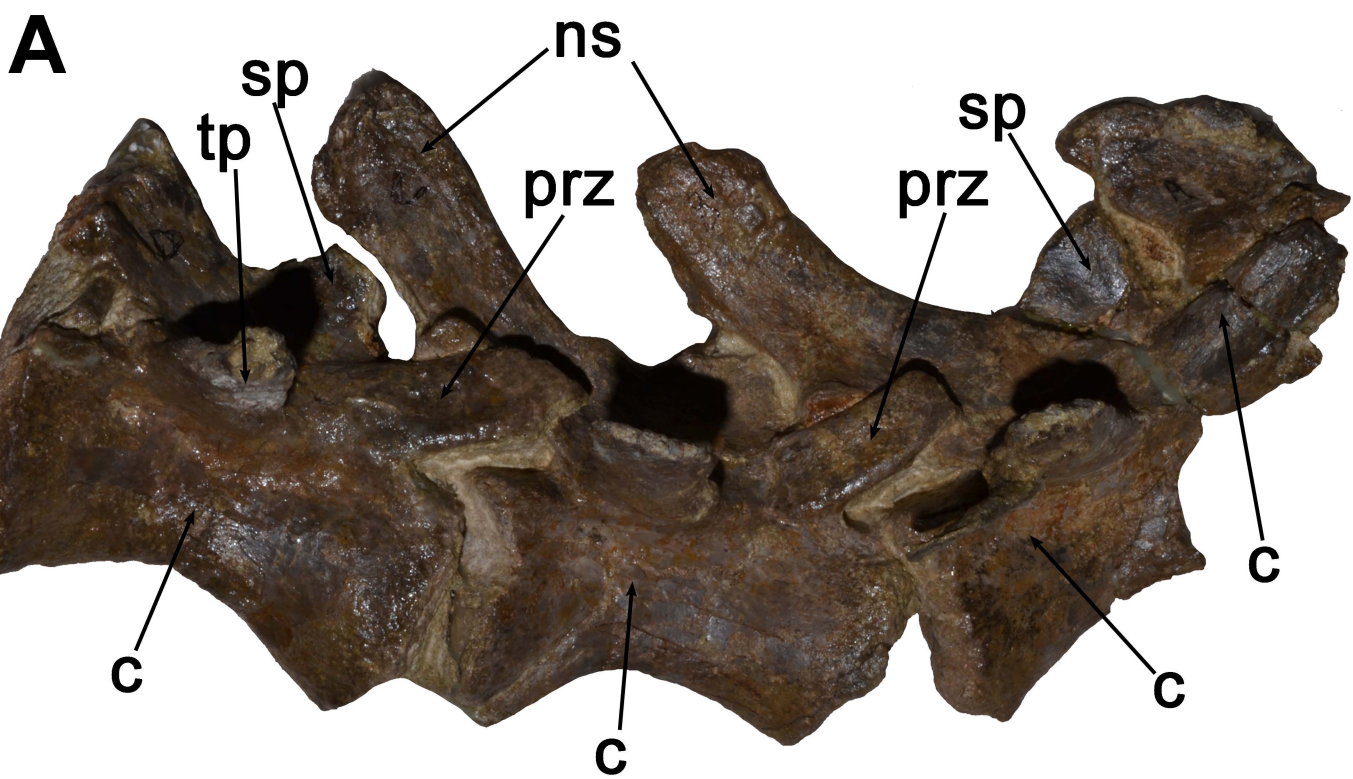




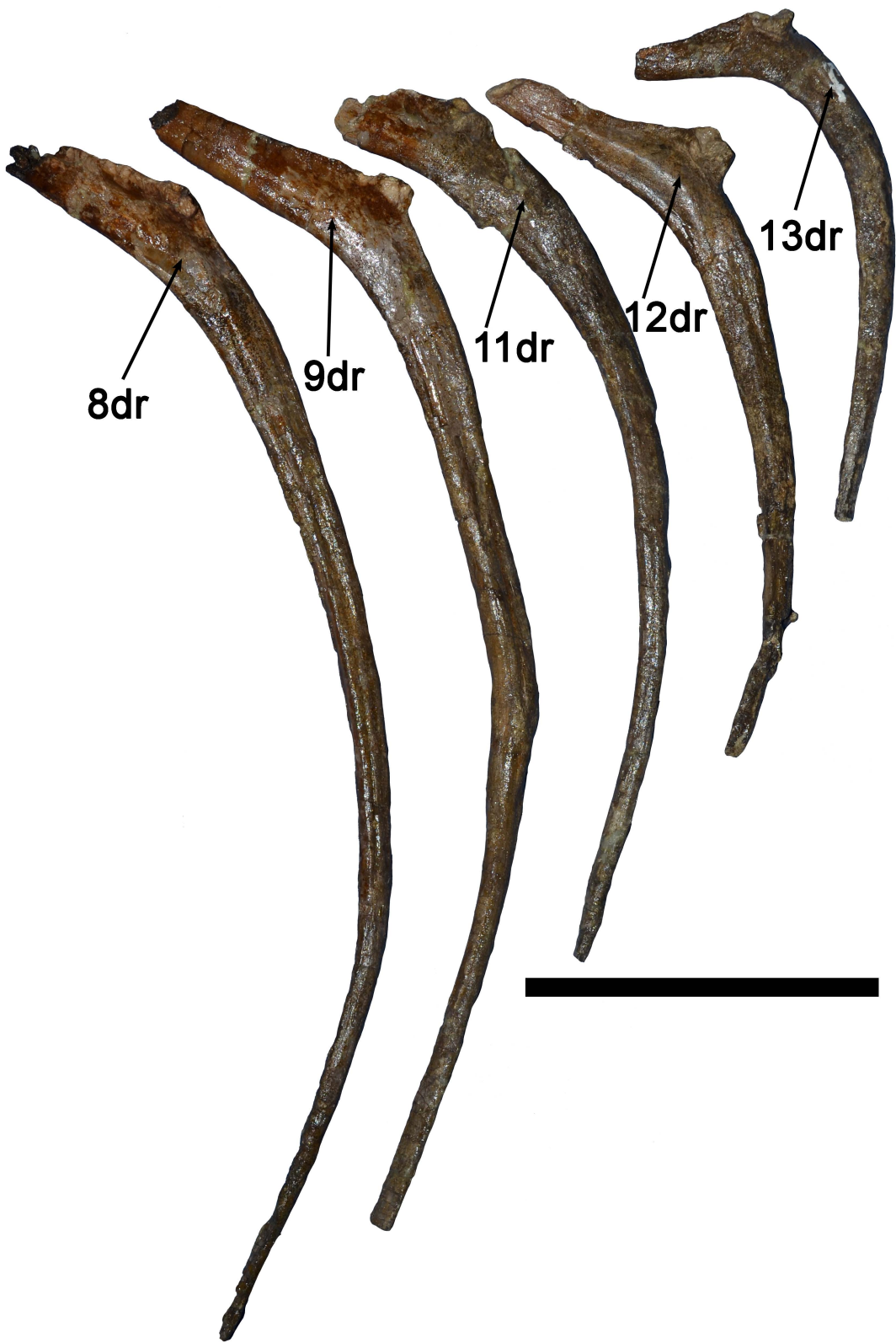












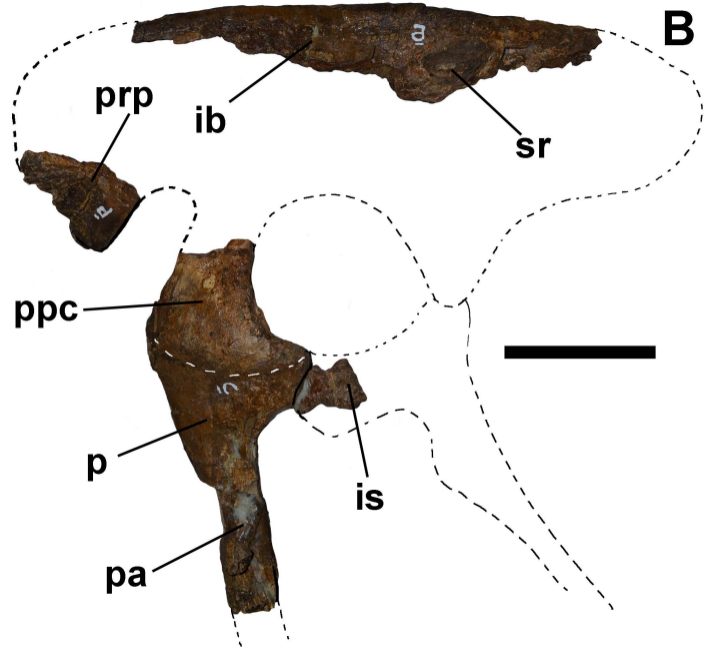
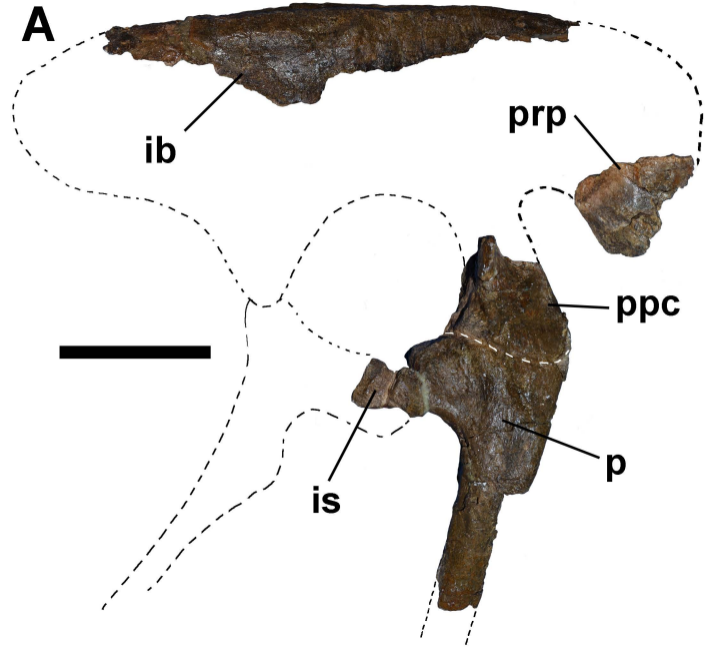
8dr

9dr

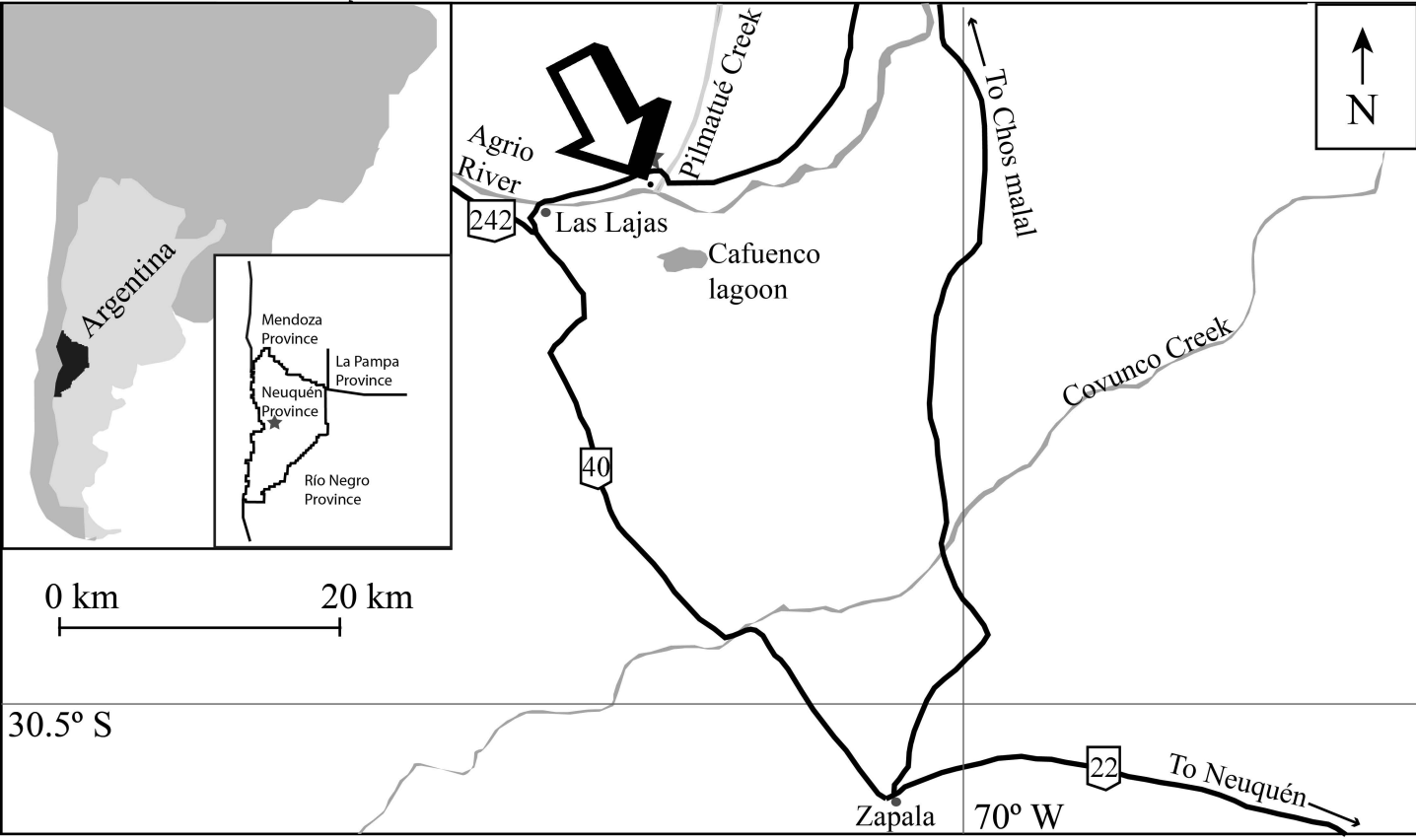
11dr

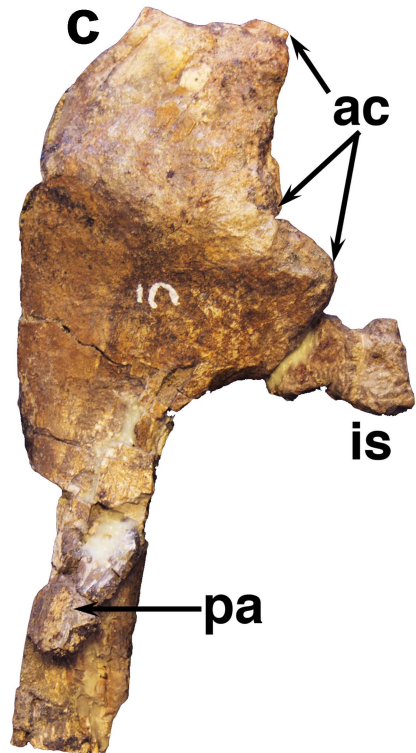
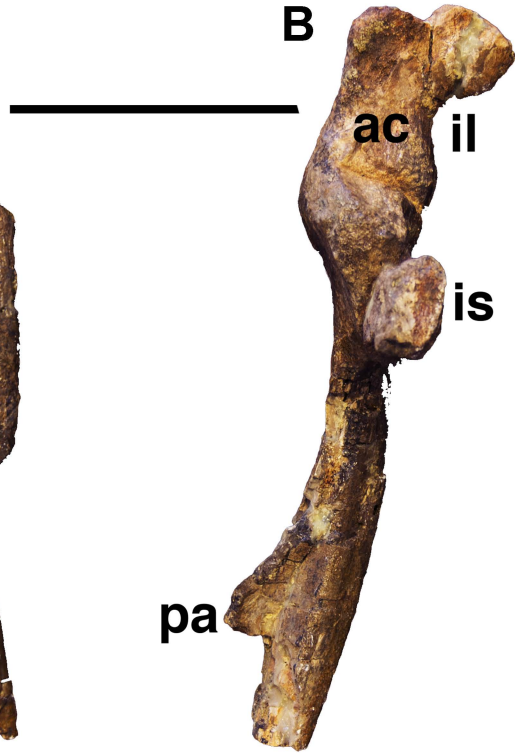
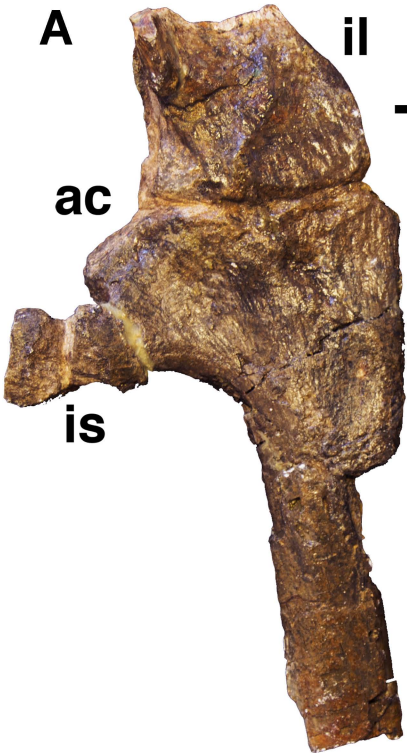
12dr

13dr

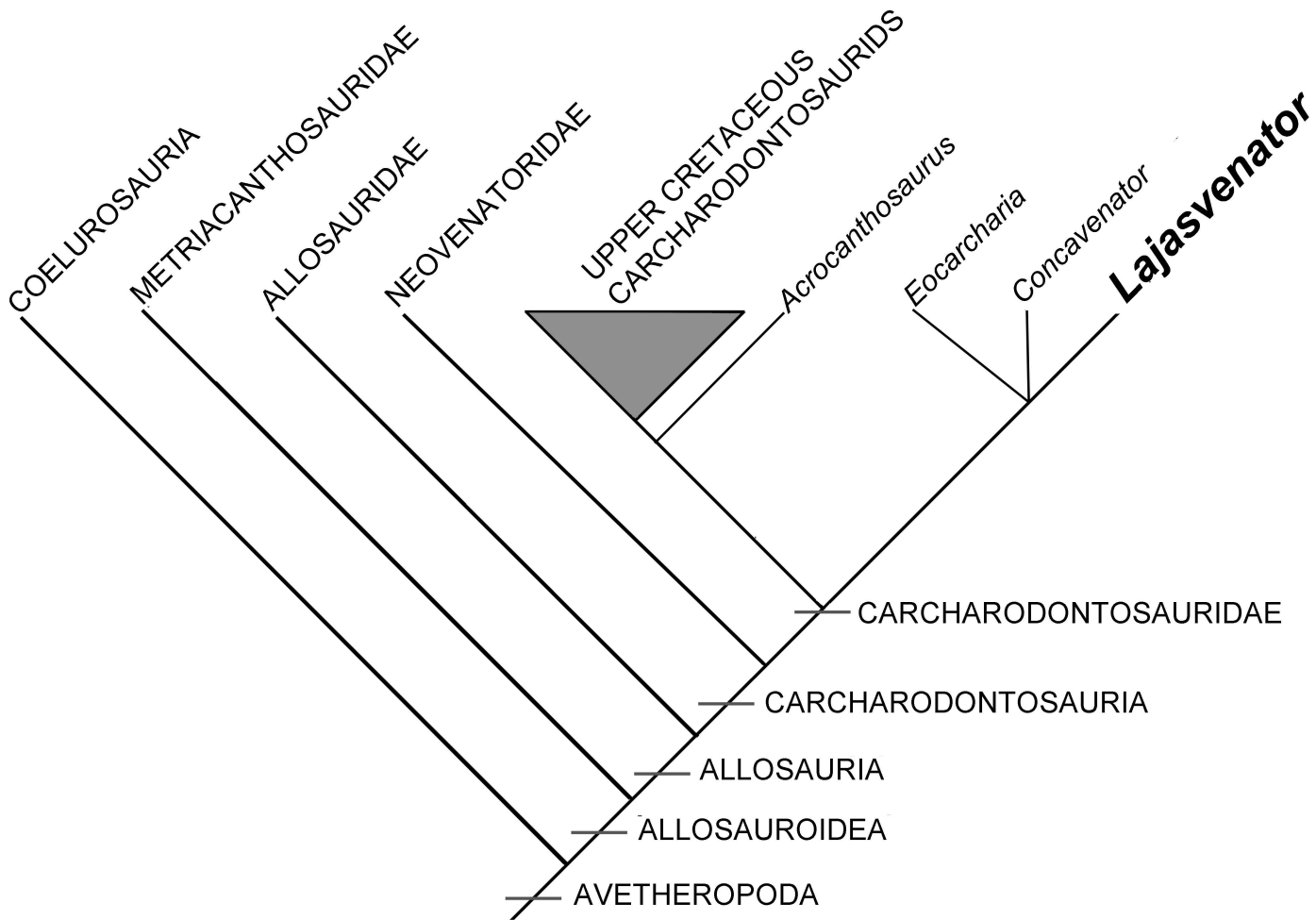


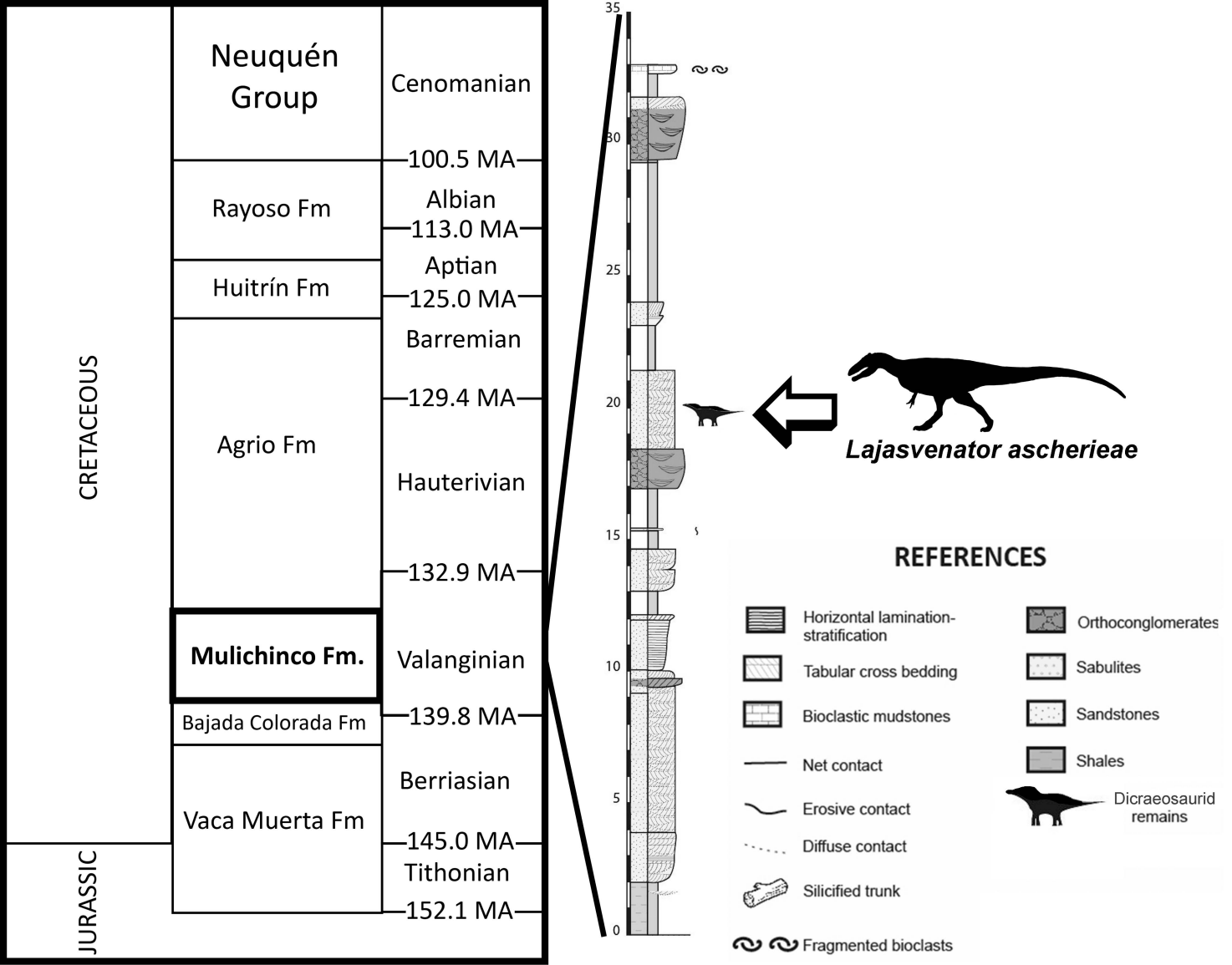


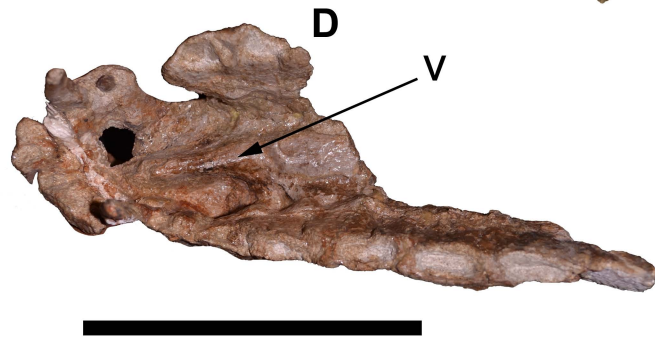
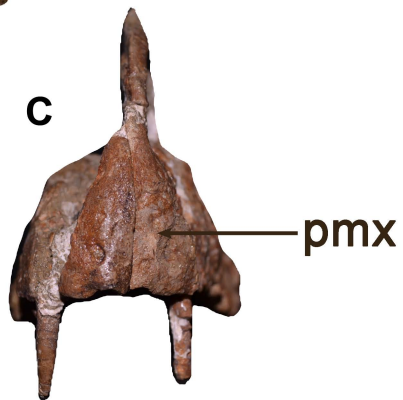
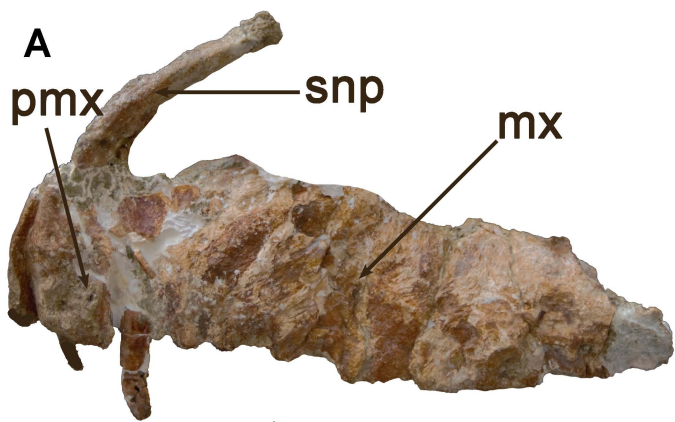


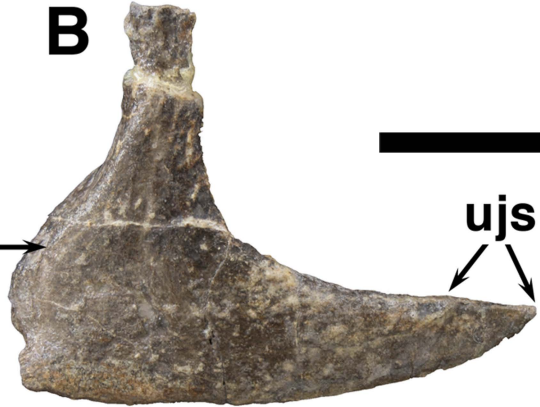
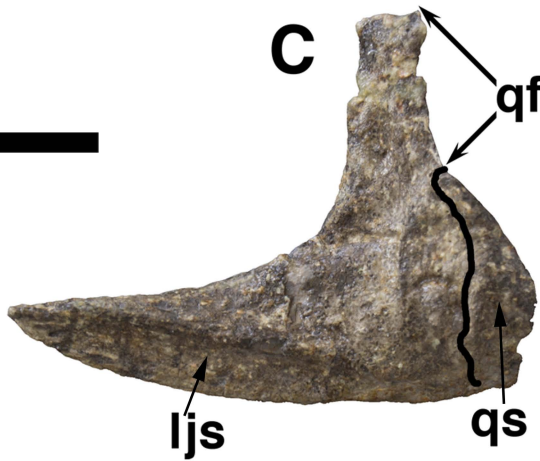


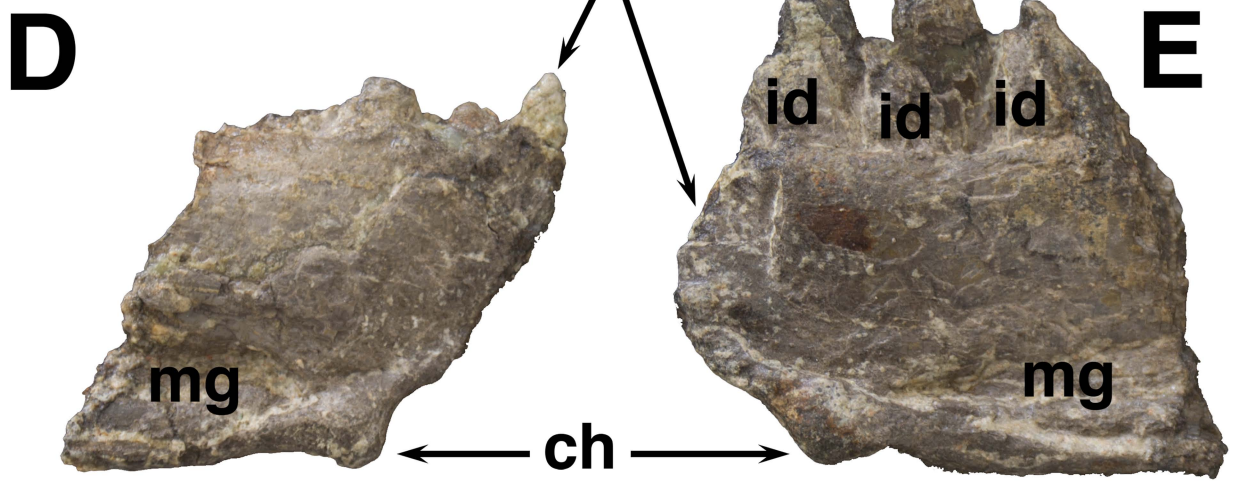
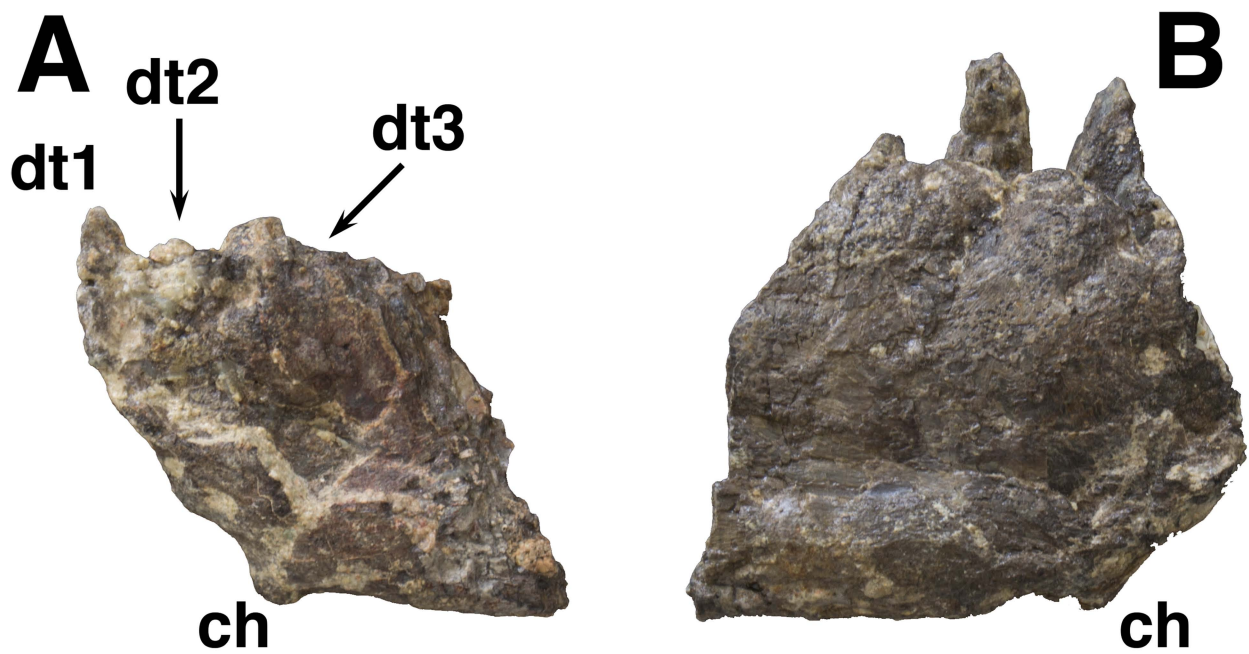




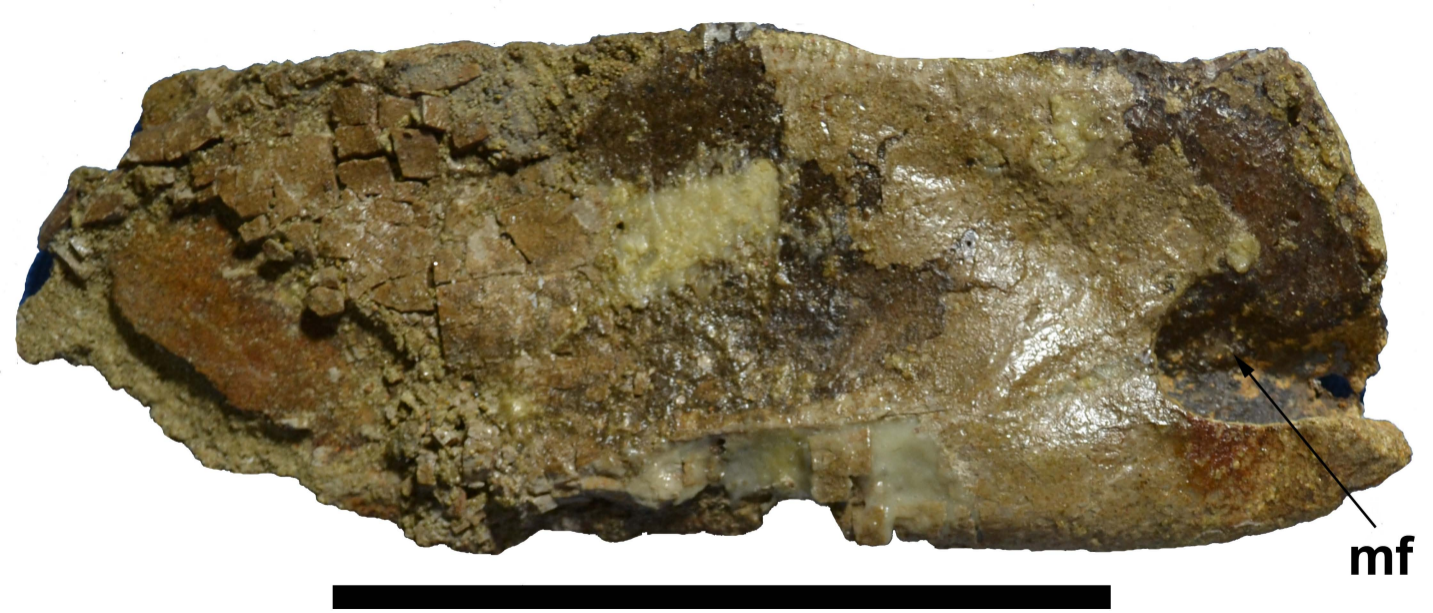




**A****qf****B****C**



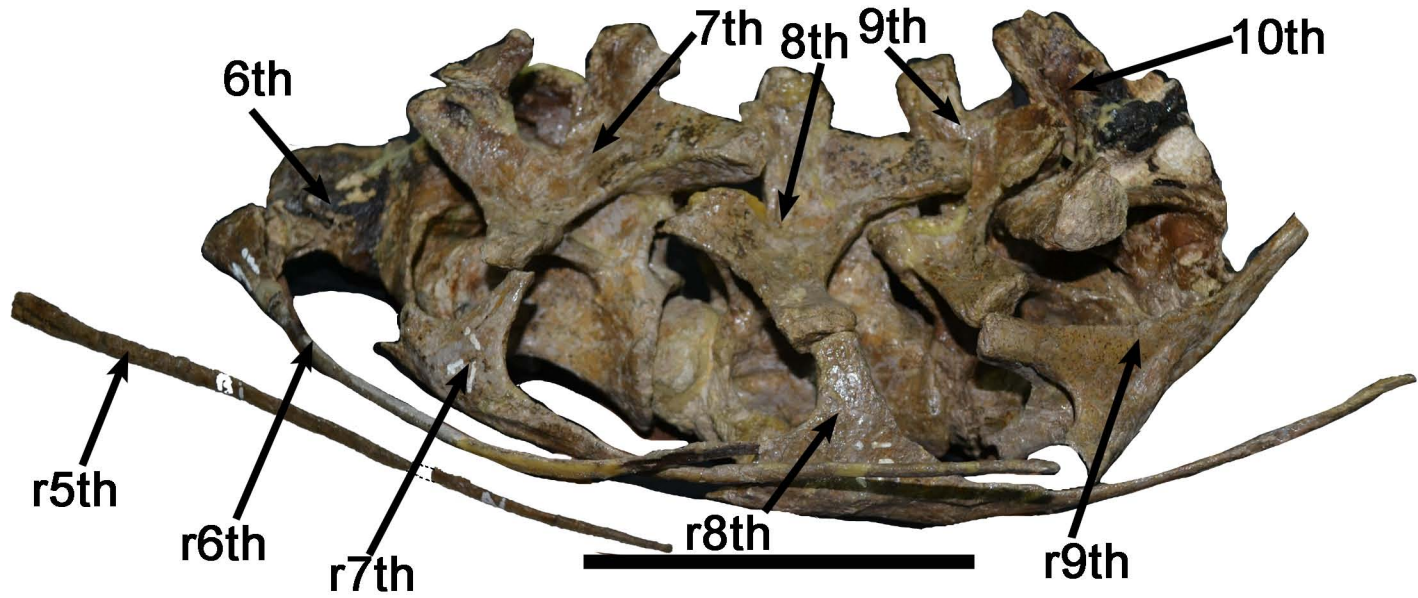




mf



aa



**Declaration of interests**

The authors declare that they have no known competing financial interests or personal relationships that could have appeared to influence the work reported in this paper.

The authors declare the following financial interests/personal relationships which may be considered as potential competing interests: